REVIEW: Atomistic mechanisms of the double proton transfer in the H-bonded nucleobase pairs: QM/QTAIM computational lessons

Article *in* Journal of biomolecular Structure & Dynamics · April 2018

DOI: 10.1080/07391102.2018.1467795

CITATIONS
5

READS
299

2 authors:

Ol'ha O Brovarets
Institute of Molecular Biology and Genetics of NAS of Ukraine, Kyiv, Ukraine
307 PUBLICATIONS **2,082** CITATIONS

SEE PROFILE

Dmytro Mykolayovych Hovorun
National Academy of Sciences of Ukraine
615 PUBLICATIONS **3,921** CITATIONS

SEE PROFILE

Journal of Biomolecular Structure and Dynamics

ISSN: 0739-1102 (Print) 1538-0254 (Online) Journal homepage: https://www.tandfonline.com/loi/tbsd20

Atomistic mechanisms of the double proton transfer in the H-bonded nucleobase pairs: QM/QTAIM computational lessons

Ol'ha O. Brovarets' & Dmytro M. Hovorun

To cite this article: Ol'ha O. Brovarets' & Dmytro M. Hovorun (2019) Atomistic mechanisms of the double proton transfer in the H-bonded nucleobase pairs: QM/QTAIM computational lessons, Journal of Biomolecular Structure and Dynamics, 37:7, 1880-1907, DOI: 10.1080/07391102.2018.1467795

To link to this article: https://doi.org/10.1080/07391102.2018.1467795

Accepted author version posted online: 20 Apr 2018.
Published online: 17 May 2018.

Journal of Biomolecular Structure and Dynamics, 2019
Vol. 37, No. 7, 1880–1907, https://doi.org/10.1080/07391102.2018.1467795

REVIEW ARTICLE

Atomistic mechanisms of the double proton transfer in the H-bonded nucleobase pairs: QM/QTAIM computational lessons

Ol'ha O. Brovarets'[a,b] and Dmytro M. Hovorun[a,b]*

[a]*Department of Molecular and Quantum Biophysics, Institute of Molecular Biology and Genetics, National Academy of Sciences of Ukraine, Kyiv, Ukraine;* [b]*Department of Molecular Biotechnology and Bioinformatics, Institute of High Technologies, Taras Shevchenko National University of Kyiv, Kyiv, Ukraine*

Communicated by Ramaswamy H. Sarma.

(*Received 31 January 2018; accepted 5 March 2018*)

In this Review, we have summarized and generalized the results of the investigation of the microstructural mechanisms of the tautomerization by the counter movement of the protons along the neighboring intermolecular H-bonds in 22 biologically important pairs of nucleotide bases in the framework of the original method, which allows to trace the evolution of the physicochemical parameters, that characterize these processes along the intrinsic reaction coordinate (IRC). It was demonstrated the performance of the introduction of the conception of the key points (KPs) (from nine to five, depending on the symmetry and nature of system), which exhaustively characterize the flow of the tautomerization processes. It was proved that for all tautomerizing base pairs the extrema of the first derivative of the electron energy of the complex by IRC coincide with the second and penultimate KPs, in which the Laplacian of the electron density equals zero at the corresponding (3,-1) bond critical points of the H-bonds. It was established the linear dependence of the width of the transition state zone of the DPT tautomerization on the degree of its asynchrony. Authors emphasize that the tautomerization reaction through the DPT of the H-bonded pairs of nucleotide bases can be considered successful in those and only in those case if the tautomerized complex is a dynamically stable system, during lifetime of which low-frequency intermolecular vibrations could develop. Perspectives of the application of the obtained approaches to the thorough study of the proton transfer processes in the biologically important objects have been briefly discussed.

Keywords: Double proton transfer; mutagenic tautomerization; intrinsic reaction coordinate; sweep of the physicochemical parameters; key point; reaction regions; transition state; reagent; product; stepwise; concerted; synchronous; asynchronous; hydrogen bond; nucleobase pair

Introduction

Proton transfer (PT), in particular multiple PT, is a widespread phenomena in many branches of life sciences, physics, chemistry, and biology (Bell, 1973; Boutis, 1992). Thus, double proton transfer (DPT), that could be realized *via* the stepwise or concerted (synchronous or asynchronous) mechanisms along the inter- or intramolecular hydrogen (H) bonds, has been comprehensively studied at the molecular level in the different biologically important complexes – canonical A·T(WC) and G·C(WC) Watson–Crick (so-called Löwdin's mechanism) (Brovarets' & Hovorun, 2014b, 2014e, 2015h; Brovarets', Kolomiets', & Hovorun, 2012; Gorb, Podolyan, Dziekonski, Sokalski, & Leszczynski, 2004; Löwdin, 1963; Roßbach & Ochsenfeld, 2017) and wobble (Brovarets', Zhurakivsky, & Hovorun, 2015; Padermshoke, Katsumoto, Masaki, & Aida, 2008) base pairs, model protein–DNA complexes (Brovarets', Yurenko, Dubey, & Hovorun, 2012; Strazewski & Tamm, 1990) and water-assisted proton transfer in nucleosides (Markova, Pejov, Stoyanova, & Enchev, 2017), that have been considered in the literature as the source of the formation of the mutagenic tautomers (Kondratyuk, Samijlenko, Kolomiets', & Hovorun, 2000; Platonov, Samijlenko, Sudakov, Kondratyuk, & Hovorun, 2005; Samijlenko, Krechkivska, Kosach, & Hovorun, 2004), determining the origin of the spontaneous point mutations, heredity, aging, and diseases (Löwdin, 1966); and also in enzymes (Eigen, 1964; Kirby, 1997) or others (Scheiner, 1994; Koch et al., 2017; Smedarchina, Siebrand, & Fernández-Ramos, 2018).

PT reactions are governed by the transition state (TS) (Hratchian & Schlegel, 2005) – stationary point on the potential energy surface with one imaginary frequency that connects the reagent and product and could proceed over or under the barrier of the reaction *via* the tunneling (Bell, 1980; Koch et al., 2017; Löwdin, 1963; Smedarchina et al., 2018), when the energy levels of proton in its initial and final states become equal. Activation barrier of the PT defines the tautomeric equilibria and kinet-

*Corresponding author. Email: d.m.hovorun@imbg.org.ua

ical parameters, e.g. lifetime and rate constants (Atkins, 1998).

However, despite the fundamental role of this reaction, the details of the course of the tautomerization reaction *via* the DPT in the pairs of nucleobases remain poorly understood.

Thus, in particular, the overwhelming majority of the authors believe that the necessary and sufficient condition for the successful tautomerization of the H-bonded pairs of nucleobases through the DPT is the presence of a local minimum on the surface of the potential (electron) energy corresponding to the tautomerized complex (Danilov & Kventsel, 1971; Florian, Hrouda, & Hobza, 1994; Gorb et al., 2004; Jacquemin, Zúñiga, Requena, & Céron-Carrasco, 2014; Romero & Hernandez, 2017; Tolosa, Sansón, & Hidalgo, 2017, 2018). At this, the question according the conditions under which these tautomers of nucleotide bases are mutagenic is not raised at all. At the same time, the amount of the biologically important pairs of nucleotide bases, studied in terms of their tautomerization *via* the DPT, remains quite limited.

At the same time, answer on this question is of outmost importance for the understanding of the microstructural mechanisms of the origin of the spontaneous point mutations in DNA, in particular – transitions and transversions. Since for a long time the emergence of this rare, but very important from the biological point of view events, is associated with the transition of the DNA bases from the main to the rare mutagenic tautomeric forms.

So, the main goal of this Review consists in the maximal generalization of the data on the DPT tautomerization in the canonical and incorrect H-bonded nucleobase pairs involving canonical nucleobases and their mutagenic analogues obtained within the framework of the elaborated by us approach for the establishment of the atomistic mechanisms of the tautomerization *via* the double counter-transfer of protons along the neighboring intermolecular hydrogen bonds in 22 biologically important pairs of nucleotide bases (Brovarets', 2010, 2015). Obtained rules could be further extended for the survey of the DPT reactions in the others biologically important complexes, not only in nucleobase pairs.

Microstructural mechanisms of the double proton transfer in the H-bonded nucleobase pairs. For the first time we have explored Löwdin's mechanism (Löwdin, 1963, 1966) of the induction of the mutagenic tautomers *via* the DPT along the neighboring intermolecular H-bonds not only for the canonical Watson–Crick (WC) A•T(WC) and G•C(WC) DNA base pairs (Löwdin, 1963), but also for the incorrect DNA base pairs – wobble G·T, short WC-like C·T, C*·C and T*·T, long WC-like A•A*, A•G, and G·G* or Watson–Crick-like A·C*, G*·T, $G{\cdot}A_{syn}$, $A^{*}{\cdot}G^{*}_{syn}$, $A^{*}{\cdot}A_{syn}$, and $G{\cdot}G^{*}_{syn}$ base mispairs. We have also considered DPT tautomerization in the base pairs by the participation of the analogues of the A DNA base: hypoxanthine (H) arising from the oxidative deamination of A (Karran & Lindahl, 1980; Kondratyuk et al., 2000) (long WC-like H•H, H*•H, H·A, and short WC-like H•C, H*•T base mispairs) and 2-aminopurine (2AP), that is a highly energetic structural isomer of A DNA base (Hovorun, 1997) and is commonly known as strong mutagen (Brovarets' & Pérez-Sánchez, 2016, 2017; Brovarets', Pérez-Sánchez, & Hovorun, 2016; Brovarets', Voiteshenko, & Hovorun, 2018; Brovarets', Voiteshenko, Pérez-Sánchez, & Hovorun, 2017a, 2018; Ronen, 1980) and fluorescent analogue (Ward, Reich, & Stryer, 1969) (T·2AP* and G·2AP* base mispairs).

Here and below, mutagenic tautomers of the nucleobases (Kondratyuk et al., 2000; Platonov et al., 2005; Samijlenko et al., 2004) are marked by the asterisks; moreover, we have used standard numeration of their atoms (Saenger, 1984).

As a results, it was established that the A•T↔A*•T* (Brovarets' & Hovorun, 2014b, 2015h), G•C↔G*•C* (Brovarets' & Hovorun, 2014e), G·T↔G*·T* (Brovarets' et al., 2015), A•G↔A*•G* (Brovarets', Zhurakivsky, & Hovorun, 2014c), C•T↔C*•T* (Brovarets' & Hovorun, 2013a), $G{\bullet}G^{*}_{syn}$↔$G^{*}{\bullet}G^{*}_{syn}$ (Brovarets' & Hovorun, 2014a), $A^{*}{\bullet}A_{syn}$↔$A{\bullet}A^{*}_{syn}$ (Brovarets', Zhurakivsky, & Hovorun, 2014b), $A^{*}{\bullet}G^{*}_{syn}$↔$A{\bullet}G^{*}_{syn}$ (Brovarets' & Hovorun, 2014c), H•C↔H*•C* (Brovarets' & Hovorun, 2013c; Brovarets', Zhurakivsky, & Hovorun, 2013a), H•H↔H*•H* (Brovarets' & Hovorun, 2013c; Brovarets' et al., 2013a) and H·A↔H*·A* (Brovarets' & Hovorun, 2013c; Brovarets', Zhurakivsky, & Hovorun, 2014d) tautomerization processes *via* the DPT are not responsible for the generation of the mutagenic tautomers, since the terminal, tautomerized base pairs are dynamically unstable: low-frequency intermolecular vibrations can't develop during their lifetime (Figure 1, Table 1). Dynamical non-stability possesses quantum nature and occurs due to the fact that the zero energy of the stretching vibration υ(AH), which frequency becomes imaginary in the TS of tautomerization, exceeds its reverse electronic barrier. The $G{\cdot}A_{syn}$ DNA base mispair does not tautomerize *via* the DPT at all, since there is no local minimum corresponding to the tautomerized $G^{*}{\cdot}A^{*}_{syn}$ mismatch on the potential energy surface (Brovarets' & Hovorun, 2014c).

At the tautomerization of the dynamically stable short WC-like T•T* (Brovarets', Zhurakivsky, & Hovorun, 2014a) and C•C* (Brovarets' & Hovorun, 2013b), as well as long WC-like A•A* (Brovarets', Zhurakivsky, & Hovorun, 2013b), G•G* (Brovarets' & Hovorun, 2014d) and H•H* (Brovarets' & Hovorun, 2013c; Brovarets', Zhurakivsky, & Hovorun, 2013c) nucleobase pairs, mutagenic tautomers are distributed among the monomers with equal probability, that is

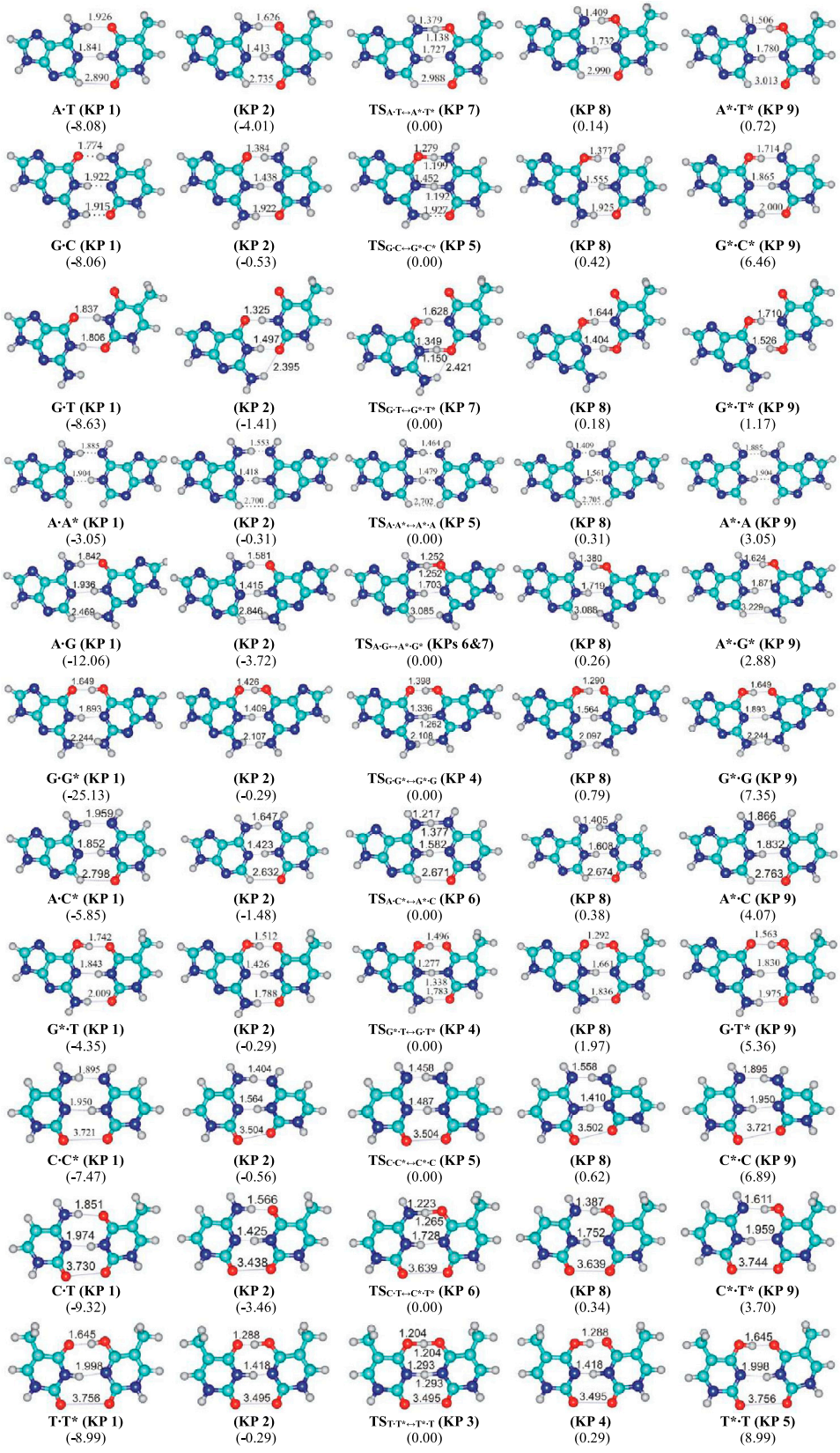

Figure 1. Geometrical structures of the five the most important key points (KPs) (numerical values of their IRC are presented below in Bohr) describing the progression of the tautomerization *via* the DPT along the intermolecular H-bonds in the investigated nucleobase pairs (B3LYP/6–311++G(d,p) level of theory, ε = 1). The dotted lines indicate AH···B, CH···B, AH···HB H-bonds and attractive A···B van der Waals contacts, while continuous lines show covalent bonds (their lengths are presented in angstroms). Carbon atoms are in light blue, nitrogen in dark blue, hydrogen in gray, and oxygen in red.

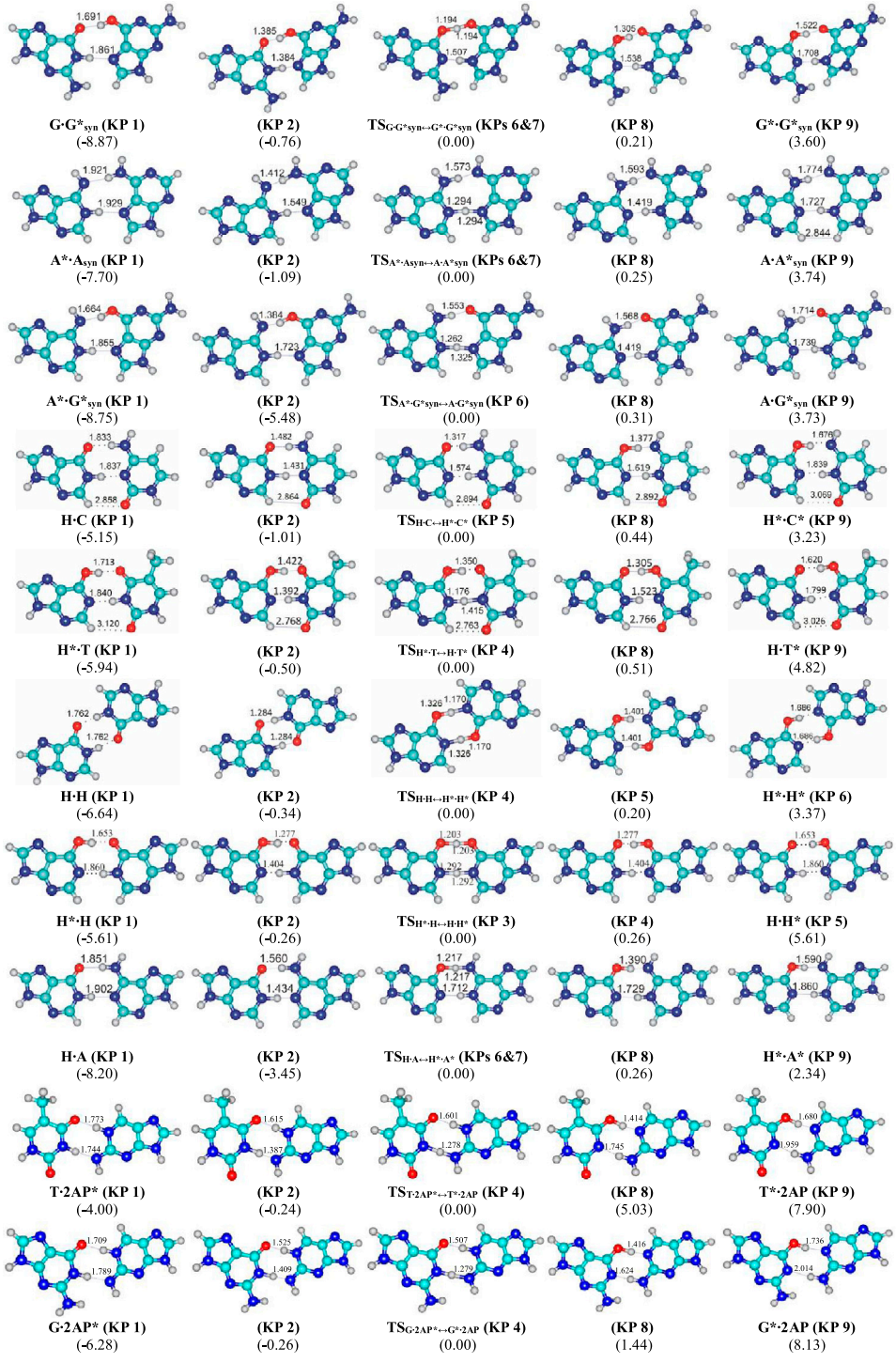

Figure 1. (*Continued*)

important for understanding of the consolidation of the point mutations – transitions and transversions – in the subsequent rounds of DNA replication (Figure 1, Table 1).

It was established that the short-lived, low-populated A*·C, G·T*, and H*•T mispairs are 'providers' of the long-lived enzymatically competent A·C* (Brovarets' & Hovorun, 2015a), G*·T (Brovarets', & Hovorun, 2015b, 2015c), and H•T* (Brovarets' & Hovorun, 2013c; Bro-

varets' et al., 2013a) base pairs, respectively, at the origin of the replication errors in DNA. Moreover, by comparison of the calculated distances of the intermolecular H-bonds with the data of the X-ray experiments (Bebenek, Pedersen, & Kunkel, 2011; Brovarets' & Hovorun, 2015a, 2015b, 2015c, 2015d; Wang, Hellinga, & Beese, 2011), it was established for the first time that the incorrect A·C and G·T base pairs with Watson–Crick geometry occur in the A·C* and G*·T tautomeric forms in the recognition pocket of the high-fidelity DNA-polymerase in its closed state.

Recently, this biologically important conclusion (Brovarets', & Hovorun, 2015b, 2015c), made by us using the simplest model systems – H-bonded pairs of nucleobases, has been confirmed by the molecular dynamics at the high molecular level (Maximoff, Kamerlin, & Florian, 2017).

Our research group have developed original methodology allowing to understand the intricacies of the atomic mechanisms of the DPT tautomerization and to obtain the evolution of the physicochemical parameters, such as electronic energy E, the first derivative of the electronic energy by the intrinsic reaction coordinate (IRC) dE/dIRC, the dipole moment of the base pair μ, the distances $d_{A\cdots B}$, $d_{AH/HB}$, and the angle ∠AH···B of the intermolecular H-bonds, the electron density ρ, the Laplacian of the electron density Δρ, ellipticity ε, and the energy E_{HB} at the (3,-1) bond critical points of the intrapair H-bonds, the NBO charges q_{NBO} of the hydrogen atoms involved in the tautomerization, the glycosidic angles α_1/α_2, and the distance $R(H_{1/9}–H_{1/9})$ between the glycosidic hydrogens, along the entire IRC, not only in the stationary structures such as reagent, product, and transition state (Brovarets', 2010, 2015; Brovarets' & Hovorun, 2013a, 2013b, 2013c, 2014a, 2014b, 2014c, 2014d, 2014e, 2015a, 2015b, 2015c, 2015d, 2015e, 2015f, 2015g, 2015h; Brovarets' et al., 2013a, 2013b, 2013c, 2014a, 2014b, 2014c, 2014d, 2015; Brovarets' & Pérez-Sánchez, 2016, 2017; Brovarets', Pérez-Sánchez, et al., 2016; Brovarets', Voiteshenko, et al., 2018; Brovarets', Voiteshenko, Pérez-Sánchez, et al., 2017a, 2017b) (Figures 1–5, 7–9, Tables 1–4).

So, based on the profiles of the geometrical parameters of the complexes and H-bonds in them, it was established that the processes of the DPT tautomerization through the counter-transfer of the protons along the antiparallel H-bonds are accompanied by the deformation or, in other words, so-called 'breathing' of the bases within pairs, in particular their compression becomes pronounced at the TS region due to the decreasing of the intermolecular distances. It was also outlined the characteristic boundaries of these geometrical changes. It was revealed that complexes compress in the process of the DPT tautomerization due to the decreasing of the distance between the monomers and also at this the mutual reorientation of the monomers takes place (Brovarets', 2010, 2015; Brovarets' & Hovorun, 2013a, 2013b, 2013c, 2014a, 2014b, 2014c, 2014d, 2014e, 2015a, 2015b, 2015c, 2015d, 2015e, 2015f, 2015g, 2015h; Brovarets' et al., 2013a, 2013b, 2013c, 2014a, 2014b, 2014c, 2014d, 2015; Brovarets' & Pérez-Sánchez, 2016, 2017; Brovarets', Pérez-Sánchez, et al., 2016; Brovarets', Voiteshenko, et al., 2018; Brovarets', Voiteshenko, Pérez-Sánchez, et al., 2017a, 2018) (Figures 8(d)–(h)).

Sweeps of the dipole moments μ along the IRC of the DPT tautomerizations convincingly demonstrate that these processes are dipole active, that is accompanied by the changes of the dipole moment of the system as by the absolute value, so by the orientation (Figure 3). This means that tautomerizing complexes emit electromagnetic energy during the DPT tautomerization. From the one side, this property of the complexes could be used for the construction of the molecular generators of the electromagnetic waves, and from the other side – this opens the possibility for the managment of these processes by the external electric fields (Arabi & Matta, 2011; Cerón-Carrasco, Cerezo, & Jacquemin, 2014; Cerón-Carrasco & Jacquemin, 2013a, 2013b; Ruiz-Blanco, Almeida, Sotomayor-Torres, & García, 2017; Shaik, Mandal, & Ramanan, 2016; Sowlati-Hashjin & Matta, 2013; Zhang & Xie, 2016).

We have also registered the case of the so-called "silent" H•H↔H*•H* (Brovarets' & Hovorun, 2013c; Brovarets' et al., 2013a) DPT tautomerization, during which the zero dipole moment of a system with C_{2h} symmetry does not change, remaining zero throughout entire reaction.

Analysis of the dependence of the NBO charges of the hydrogen atoms, migrating along the neighboring intermolecular H-bonds during the tautomerization of the complexes, on the IRC enables us to arrive to the conclusion that protons participating in these processes do not go beyond their electronic coat and transfer as hydrogen atoms (Brovarets', 2010, 2015; Brovarets' & Hovorun, 2013a, 2013b, 2013c, 2014a, 2014b, 2014c, 2014d, 2014e, 2015a, 2015b, 2015c, 2015d, 2015e, 2015f, 2015g, 2015h; Brovarets' et al., 2013a, 2013b, 2013c, 2014a, 2014b, 2014c, 2014d, 2015; Brovarets' & Pérez-Sánchez, 2016, 2017; Brovarets', Pérez-Sánchez, et al., 2016; Brovarets', Voiteshenko, et al., 2018; Brovarets', Voiteshenko, Pérez-Sánchez, et al., 2017a, 2018).

Based on the electron-topological characteristics of the neighboring intermolecular bonds, along which protons migrate, namely the value of the electron density ρ and its Laplacian Δρ in the corresponding bond critical points (Bader, 1990), in particular on the crossings of their curves and the points, where they become zeros, for the first time we have introduced the conception of the key points (KPs) (their maximum number in accordance with the rules of their introduction reaches 9),

Table 1. Energetic and kinetic characteristics of the tautomeric transformations of the canonical Watson-Crick, wobble, incorrect long, short, and Watson–Crick-like pairs of nucleotide bases *via* the DPT along the neighboring intermolecular H-bonds in the free state.

N	Tautomerization reaction *via* the DPT	Number of KPs	Type of tautomerization reaction	ΔG^a	ΔE^b	$\Delta\Delta G_{TS}{}^c$	$\Delta\Delta E_{TS}{}^d$	$\Delta\Delta G^e$	$\Delta\Delta E^f$	τ^g
MP2/aug-cc-pVTZ//MP2/6–311++G(d,p)										
1	A·T↔A*·T* (Brovarets' & Hovorun, 2014b, 2015h)	9	Asynchronous concerted	11.95	12.26	10.29	12.40	−1.66	0.14	$6.5\cdot10^{-15}$
2	G·C↔G*·C* (Brovarets' & Hovorun, 2014e)	9	Asynchronous concerted	9.22	8.22	9.69	13.28	0.47	5.06	$1.6\cdot10^{-13}$
MP2/cc-pVQZ//B3LYP/6–311++G(d,p)										
3	G·T↔G*·T* (Brovarets' et al., 2015)	9	Asynchronous concerted	11.28	12.30	10.20	12.76	−1.09	0.46	$2.2\cdot10^{-14}$
4	A·A*↔A*·A (Brovarets', Zhurakivsky, & Hovorun, 2013b)	9	Synchronous concerted	0.00	0.00	7.01	10.33	7.01	10.33	$1.8\cdot10^{-8}$
5	A·G↔A*·G* (Brovarets' et al., 2014c)	8	Asynchronous concerted	10.07	9.58	9.63	11.46	−0.44	1.88	$4.8\cdot10^{-14}$
6	G·G*↔G*·G (Brovarets' & Hovorun, 2014d)	9	Asynchronous concerted	0.00	0.00	5.51	8.33	5.51	8.33	$8.2\cdot10^{-10}$
7	A·C*↔A*·C (Brovarets' & Hovorun, 2015a)	9	Asynchronous concerted	3.99	3.64	8.17	10.53	4.18	6.89	$1.1\cdot10^{-10}$
8	G*•T↔G•T* (Brovarets', & Hovorun, 2015b, 2015c)	9	Asynchronous concerted	1.22	1.19	2.63	5.61	2.63	5.61	$8.1\cdot10^{-13}$
9	C·C*↔C*·C (Brovarets' & Hovorun, 2013b)	9	Asynchronous concerted	0.00	0.00	8.28	10.83	8.28	10.83	$1.5\cdot10^{-7}$
10	C·T↔C*·T* (Brovarets' & Hovorun, 2013a)	9	Asynchronous concerted	9.15	8.99	9.55	11.38	0.40	2.39	$2.1\cdot10^{-13}$
11	T·T*↔T*·T (Brovarets' et al., 2014a)	5	Synchronous concerted	0.00	0.00	4.64	8.18	4.64	8.18	$1.6\cdot10^{-10}$
12	$G\cdot G^*_{syn}\leftrightarrow G^*\cdot G^*_{syn}$ (Brovarets' & Hovorun, 2014a)	8	Asynchronous concerted	11.02	11.15	9.07	12.17	−1.96	1.02	$4.1\cdot10^{-15}$
13	$A^*\cdot A_{syn}\leftrightarrow A\cdot A^*_{syn}$ (Brovarets' et al., 2014b)	8	Asynchronous concerted	13.98	14.71	14.15	16.43	0.16	1.72	$1.1\cdot10^{-13}$
14	$A^*\cdot G^*_{syn}\leftrightarrow A\cdot G^*_{syn}$ (Brovarets' & Hovorun, 2014c)	9	Asynchronous concerted	1.89	2.20	2.42	4.60	0.52	2.40	$2.2\cdot10^{-13}$
15	H·C↔H*·C* (Brovarets' & Hovorun, 2013c; Brovarets' et al., 2013a)	9	Asynchronous concerted	6.83	6.74	8.39	11.06	1.57	4.32	$1.9\cdot10^{-12}$
16	H*·T↔H·T* (Brovarets' & Hovorun, 2013c; Brovarets' et al., 2013a)	9	Asynchronous concerted	2.94	2.67	4.75	7.75	1.82	5.07	$2.7\cdot10^{-12}$
17	H·H↔H*·H* (Brovarets' & Hovorun, 2013c; Brovarets' et al., 2013a)	6	Asynchronous concerted	5.68	6.01	5.57	9.62	−0.11	3.61	$6.6\cdot10^{-14}$
18	H*·H↔H·H* (Brovarets' & Hovorun, 2013c; Brovarets', Zhurakivsky, & Hovorun, 2013c)	5	Synchronous concerted	0.00	0.00	2.87	7.27	2.87	7.27	$8.2\cdot10^{-12}$
19	H·A↔H*·A* (Brovarets' & Hovorun, 2013c; Brovarets' et al., 2014d)	9	Asynchronous concerted	10.32	10.20	9.52	11.78	−0.80	1.58	$2.7\cdot10^{-14}$
20	T·2AP*↔T*·2AP (Brovarets' & Pérez-Sánchez, 2016; Brovarets' et al., 2017a)	9	Asynchronous concerted	−7.83	−7.50	−0.82	1.64	7.02	9.14	$1.1\cdot10^{-8}$
21	G·2AP*↔G*·2AP (Brovarets' & Pérez-Sánchez, 2016; Brovarets' et al., 2017a)	9	Asynchronous concerted	−10.70	−9.96	−0.11	2.31	10.59	12.26	$4.5\cdot10^{-6}$

[a]The Gibbs free energy of the product relatively the reactant of the tautomerization reaction (T = 298.15 K), kcal•mol^{-1}.
[b]The electronic energy of the product relatively the reactant of the tautomerization reaction, kcal•mol^{-1}.
[c]The Gibbs free energy barrier for the forward reaction of tautomerization, kcal•mol^{-1}.
[d]The electronic energy barrier for the forward reaction of tautomerization, kcal•mol^{-1}.
[e]The Gibbs free energy barrier for the reverse reaction of tautomerization, kcal•mol^{-1}.
[f]The electronic energy barrier for the reverse reaction of tautomerization, kcal•mol^{-1}.
[g]The lifetime of the product of the tautomerization reaction, s.

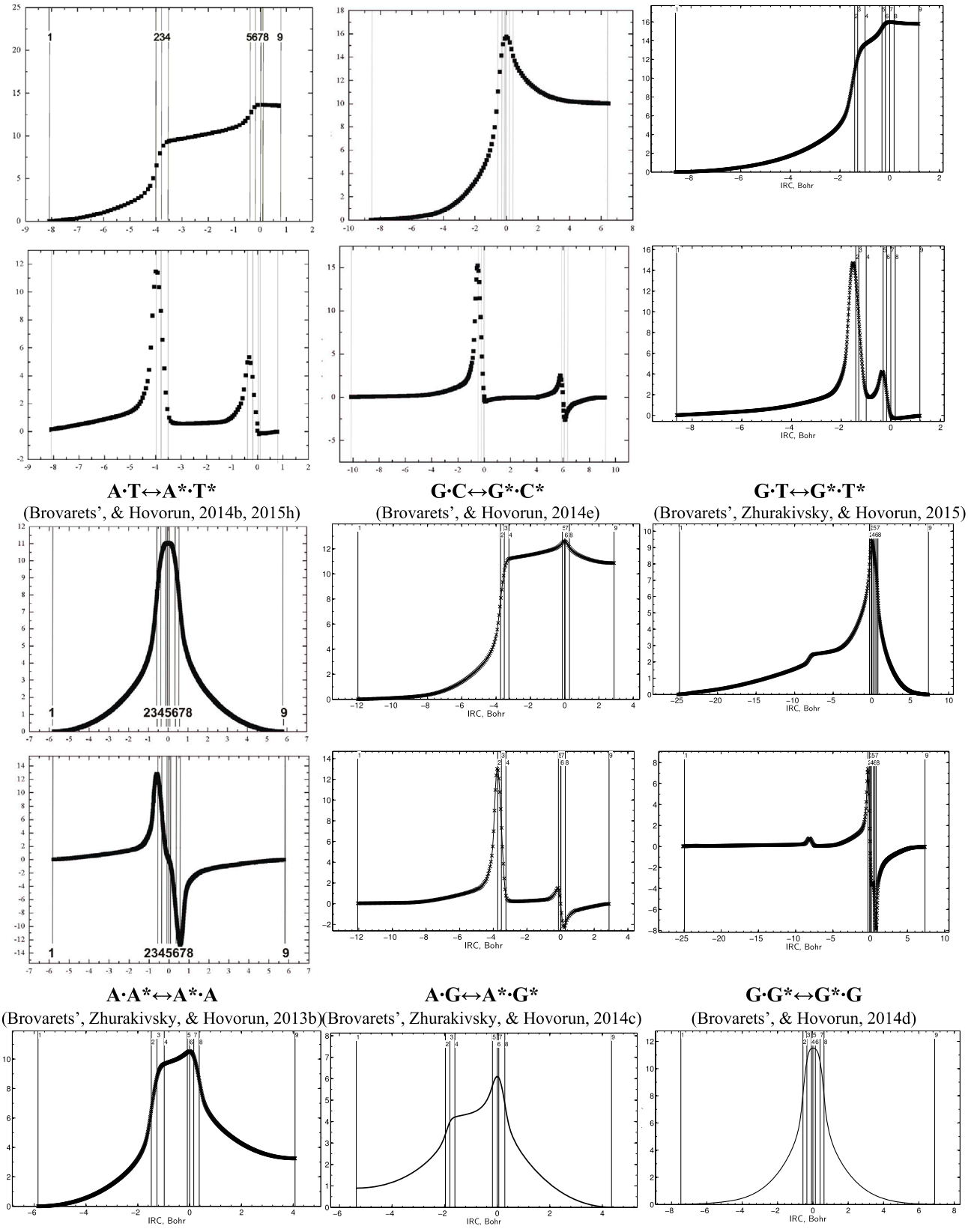

Figure 2. Profiles of the electronic energy E (upper row) (in kcal•mol^{-1}) and the first derivative of the electronic energy with respect to the IRC dE/dIRC (lower row) along the IRC of the tautomerization reactions *via* the DPT obtained at the B3LYP/6–311++G(d,p) level of theory in the free state. All key points as vertical lines are presented for each profile.

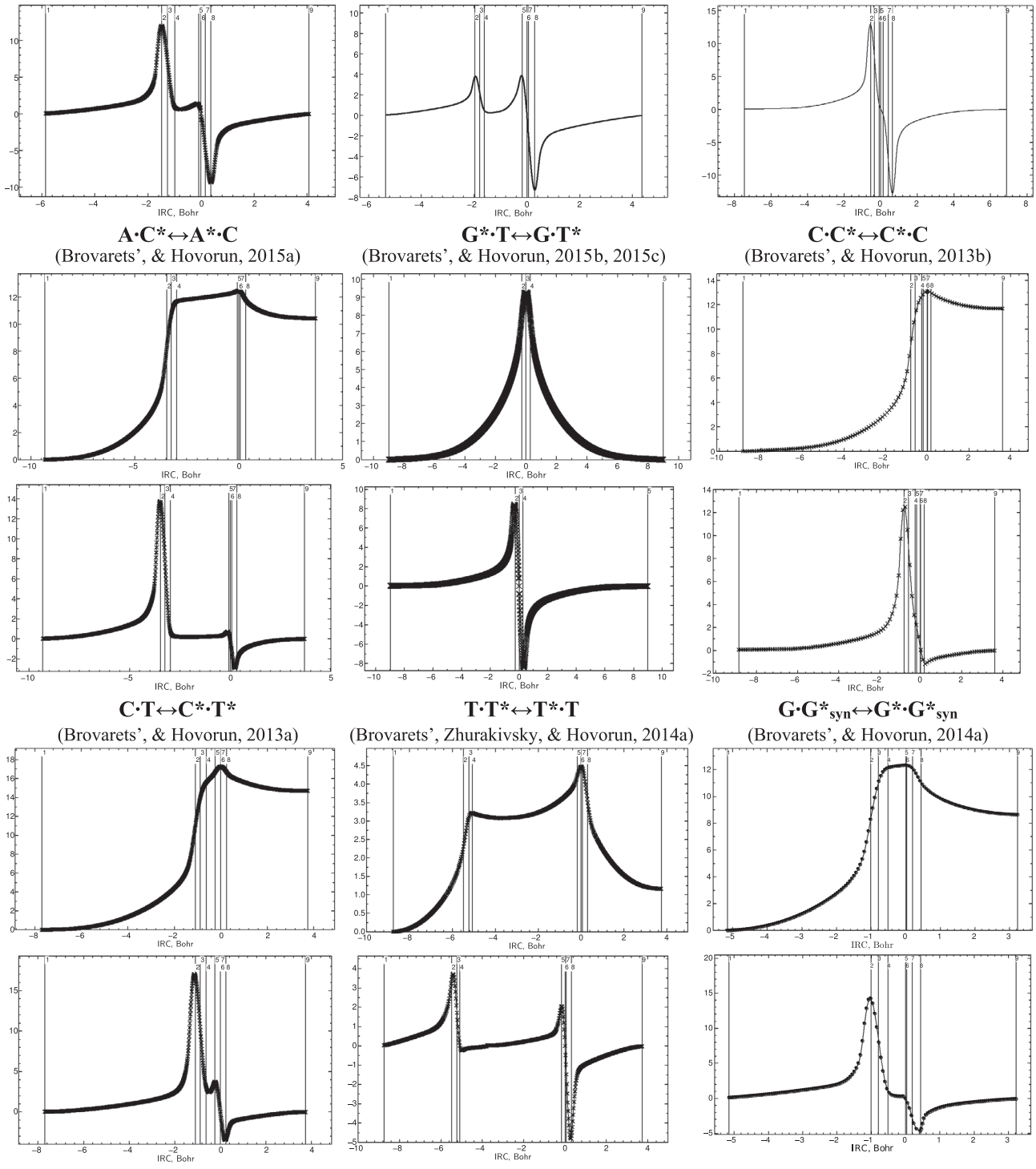

A·C*↔A*·C
(Brovarets', & Hovorun, 2015a)

G*·T↔G·T*
(Brovarets', & Hovorun, 2015b, 2015c)

C·C*↔C*·C
(Brovarets', & Hovorun, 2013b)

C·T↔C*·T*
(Brovarets', & Hovorun, 2013a)

T·T*↔T*·T
(Brovarets', Zhurakivsky, & Hovorun, 2014a)

G·G*$_{syn}$↔G*·G*$_{syn}$
(Brovarets', & Hovorun, 2014a)

A*·A$_{syn}$↔A·A*$_{syn}$
(Brovarets', Zhurakivsky, & Hovorun, 2014b)

A*·G*$_{syn}$↔A·G*$_{syn}$
(Brovarets', & Hovorun, 2014c)

H·C↔H*·C*
(Brovarets', & Hovorun, 2013c; Brovarets', Zhurakivsky, & Hovorun, 2013a)

Figure 2. (*Continued*)

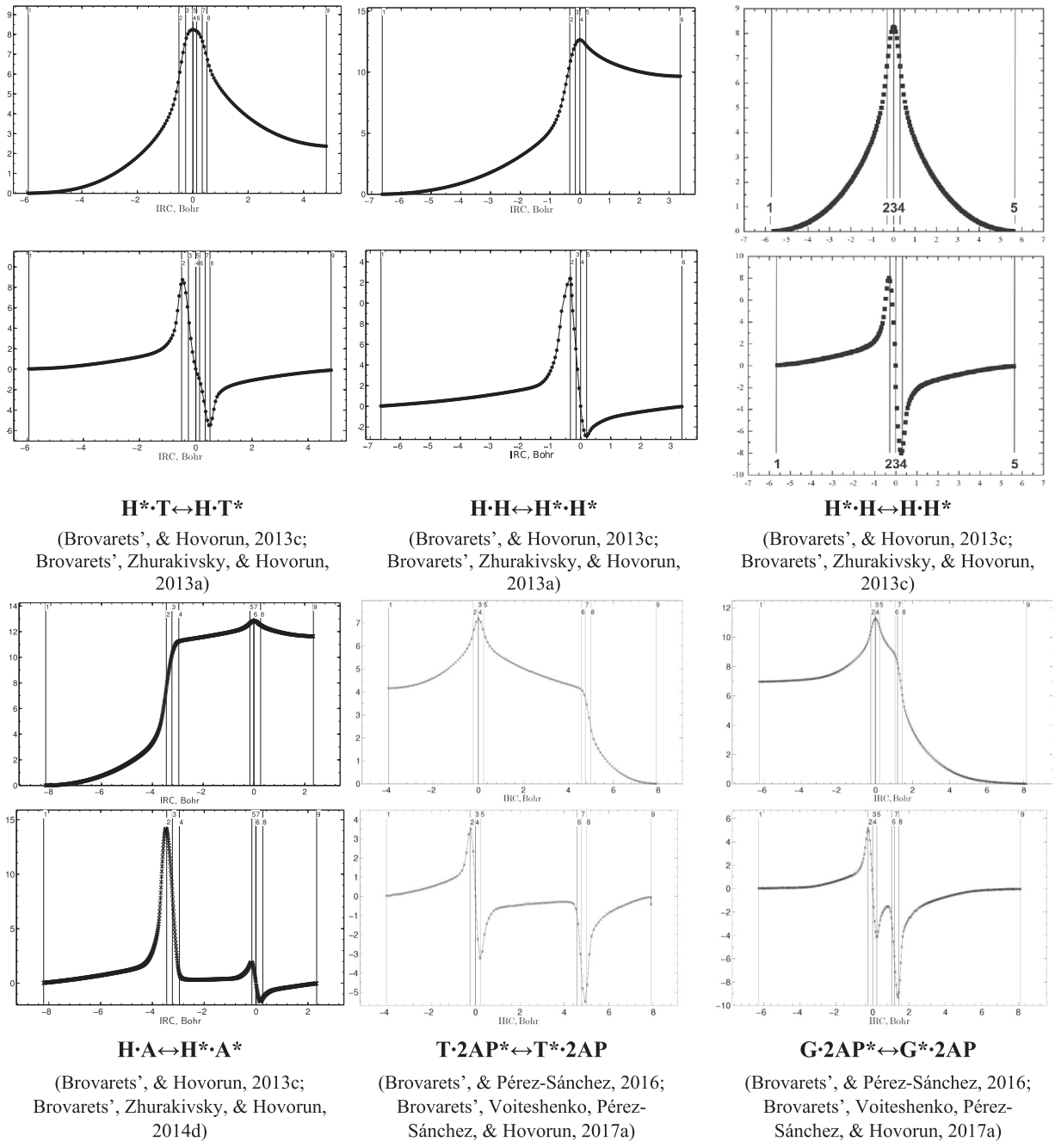

H*·T↔H·T*

(Brovarets', & Hovorun, 2013c; Brovarets', Zhurakivsky, & Hovorun, 2013a)

H·H↔H*·H*

(Brovarets', & Hovorun, 2013c; Brovarets', Zhurakivsky, & Hovorun, 2013a)

H*·H↔H·H*

(Brovarets', & Hovorun, 2013c; Brovarets', Zhurakivsky, & Hovorun, 2013c)

H·A↔H*·A*

(Brovarets', & Hovorun, 2013c; Brovarets', Zhurakivsky, & Hovorun, 2014d)

T·2AP*↔T*·2AP

(Brovarets', & Pérez-Sánchez, 2016; Brovarets', Voiteshenko, Pérez-Sánchez, & Hovorun, 2017a)

G·2AP*↔G*·2AP

(Brovarets', & Pérez-Sánchez, 2016; Brovarets', Voiteshenko, Pérez-Sánchez, & Hovorun, 2017a)

Figure 2. (*Continued*)

which comprehensively describe the mechanism of tautomerization and are figuratively speaking the "fingerprints" of these reactions (Brovarets', 2010, 2015; Brovarets' & Hovorun, 2013a, 2013b, 2013c, 2014a, 2014b, 2014c, 2014d, 2014e, 2015a, 2015b, 2015c, 2015d, 2015e, 2015f, 2015g, 2015h; Brovarets' et al., 2013a, 2013b, 2013c, 2014a, 2014b, 2014c, 2014d, 2015; Brovarets' & Pérez-Sánchez, 2016, 2017; Brovarets', Pérez-Sánchez, et al., 2016; Brovarets', Voiteshenko, et al., 2018; Brovarets', Voiteshenko, Pérez-Sánchez, et al., 2017a, 2018) (Figures 1, 7, 8, Table 4).

Three KPs correspond to the stationary points on the potential energy surface: two local minima – reagent (the 1st KP), product (the last KP), and the transition state of the DPT tautomerization. Others six KPs include: two KPs (third and seventh for the biologically important A•C*↔A*•C tautomerization *via* the DPT (Figures 7, 8, Table 4)), in which migrating proton is localized midway

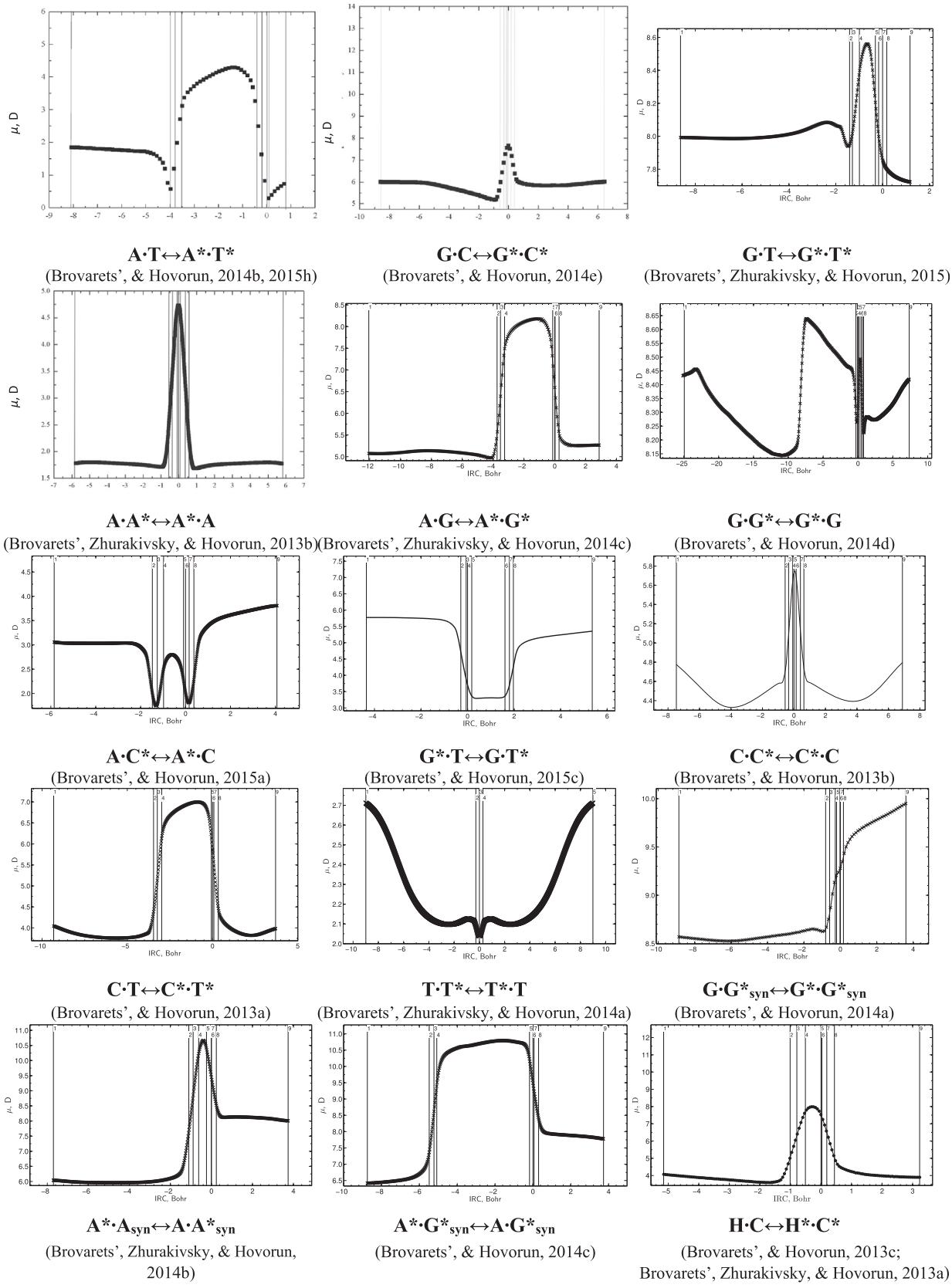

Figure 3. Profile of the dipole moment μ (in Debay) along the IRC of the tautomerization reactions *via* the DPT obtained at the B3LYP/6–311++G(d,p) level of theory in the free state. All key points as vertical lines are presented for each profile.

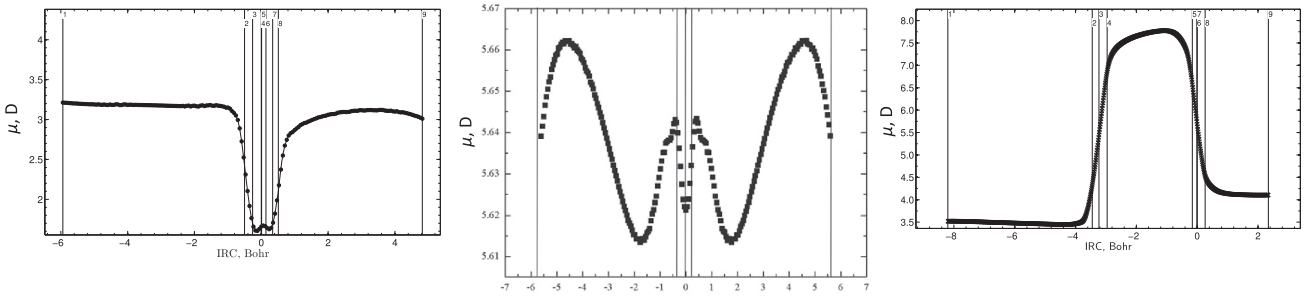

H*·T↔H·T*
(Brovarets', & Hovorun, 2013c; Brovarets', Zhurakivsky, & Hovorun, 2013a)

H·H↔H*·H*
(Brovarets', & Hovorun, 2013c; Brovarets', Zhurakivsky, & Hovorun, 2013a)

H·A↔H*·A*
(Brovarets', & Hovorun, 2013c; Brovarets', Zhurakivsky, & Hovorun, 2014d)

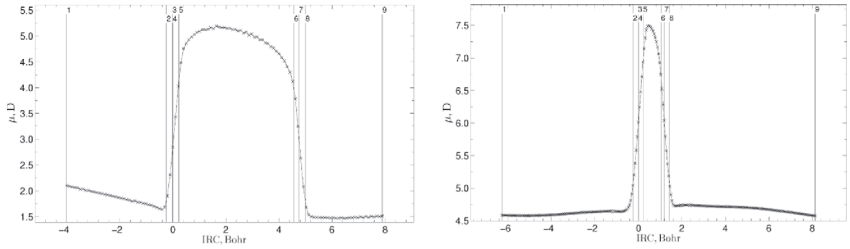

T·2AP*↔T*·2AP
(Brovarets', & Pérez-Sánchez, 2016; Brovarets', Voiteshenko, Pérez-Sánchez, & Hovorun, 2017a)

G·2AP*↔G*·2AP
(Brovarets', & Pérez-Sánchez, 2016; Brovarets', Voiteshenko, Pérez-Sánchez, & Hovorun, 2017a)

Figure 3. (*Continued*)

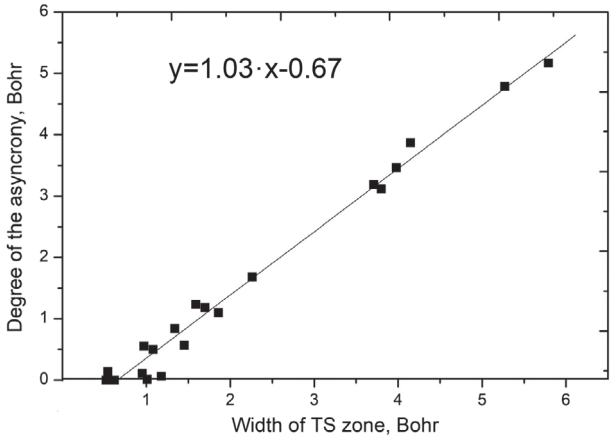

Figure 4. Dependency of the degree of the asynchrony on the width of the TS zone obtained at the B3LYP/6–311++G(d,p) level of theory in the free state (see Table 3).

between the electronegative atoms and are characterized by the loosened A–H–B covalent bridge with equalized geometrical and electron-topological properties, and also four KPs (second, fourth, sixth, and eighth for the biologically important A•C*↔A*•C tautomerization *via* the DPT (Figures 7, 8, Table 4)), in which H-bonds begin to acquire the features of the covalent bond and *vice versa*, that is where the Laplacian of the electron density Δρ passes through zero – $\Delta\rho_{A\cdots H}/\Delta\rho_{H\cdots B} = 0$ (see, at the example of the biologically important A•C*↔A*•C tautomerization *via* the DPT (Figures 7, 8, Table 4)). Notably, for all considered nucleobase pairs, the profiles of the electron density ρ and its Laplacian Δρ in the (3,-1) bond critical points and also distance $d_{AH/HB}$ between the hydrogen and electronegative A or B atoms demonstrate χ-crossed curves (Figures 8(a), (b) and (e)).

It is obvious, that within the framework of the proposed by us approach the number of the KPs could not exceed nine by their definition. At the same time, we have revealed the cases, where the DPT tautomerization process is described by the smaller number of KPs, i.e. it takes place their degeneration or overlapping with each other (Figures 1, 2, 3).

In four cases – A•G↔A*•G* (Brovarets' et al., 2014c), G•G*$_{syn}$↔G*•G*$_{syn}$ (Brovarets' & Hovorun, 2014a), A*•A$_{syn}$↔A•A*$_{syn}$ (Brovarets' et al., 2014b), and H·A↔H*·A* (Brovarets' & Hovorun, 2013c; Brovarets' et al., 2014d) tautomerizations *via* the DPT – we

have registered accidental degeneration of the sixth and seventh KPs into one single KP corresponding to the TS of these reactions, that is not connected with the symmetry of the system (Figure 1, Tables 1–3). Moreover, we have registered the degeneration of the KPs from nine to five (it is obviously their minimum number), connected with the symmetry of the system. It should be honestly noted that our knowledge about the ratio between the chemistry and system symmetry of the reaction, which ultimately determines the final number of KPs, remains limited. This can be illustrated by several interesting examples.

By analogy with the H*•H↔H•H* (Brovarets' & Hovorun, 2013c; Brovarets', Zhurakivsky, & Hovorun, 2013c) and T•T*↔T*•T (Brovarets' et al., 2014a) tautomerization processes *via* the DPT it could be assumed that the A•A*↔A*•A (Brovarets', Zhurakivsky, & Hovorun, 2013b), G•G*↔G*•G (Brovarets' & Hovorun, 2014d), and C•C*↔C*•C (Brovarets' & Hovorun, 2013b) tautomerization processes *via* the DPT also would be synchronous and described by the five KPs, but these hopes were in vain (Figure 1, Tables 2, 3). Obviously, more painstaking and hard work should be done in this direction for the better understanding of the details.

The analysis of the reaction force – the first derivative of the electronic energy E by IRC was proposed in the literature (Duarte, Vöhringer-Martinez, & Toro-Labbé, 2011; Guzmán-Angel, Inostroza-Rivera, Gutiérrez-Oliva, Herrera, & Toro-Labbé, 2016; Hargis, Vöhringer-Martinez, Woodcock, Toro-Labbé, & Schaefer, 2011; Inostroza-Rivera et al., 2015; Jaque, Toro-Labbé, Politzer, & Geerlings, 2008) for the characterization of the course of the reaction and also for the partition of the entire reaction region to the three regions – reactant, transition state, and product regions. In order to characterize the electronic activity taking place during a chemical reaction within the framework of the reaction force analysis it was also proposed conceptions of the electronic chemical potential and reaction electronic flux (for more details see (Murray, Toro-Labbé, Clark, & Politzer, 2009; Politzer, Murray, & Jaque, 2013; Toro-Labbé, Gutierrez-Oliva, Concha, Murray, & Politzer, 2004; Toro-Labbé, Gutiérrez-Oliva, Murray, & Politzer, 2009; Yepes, Murray, Politzer, & Jaque, 2012; Yepes et al., 2013a, 2013b)).

Calculations of the dE/dIRC enable us to establish that these curves attain their maximum and minimum values precisely at the second and eighth/penultimate KPs (Figure 2). Basing on this, we proceed to precisely divide the whole region of the reaction pathway of these reactions to the regions of the reagent (between KPs first and second, where the H-bonds transform into the covalent bonds and *vice*), transition state (between KPs second and eighth/penultimate) and product (between KPs eighth/penultimate and ninth/terminal, where the reaction complex relaxes into the terminal complex). This enables us to interpret the phenomenology of the dE/dIRC function, that is to transfer from the phenomenological description of the reaction to the penetration into its atomic nature. It has been revealed, that the most intensive changes occur at the TS region – mutual reorientation of the bases relative to each other, proton transfer followed by the loss of the individual properties of the nucleotide bases being bound by covalent or strong electrostatic interactions, electronic and structural rebuilding of the complexes and bases within them, formation and disruption of the intermolecular covalent or hydrogen bonds (Figures 8(d)–(h)).

By analysis of the quantitative data, presented in Table 3, we have obtained for the first time the linear dependence of the degree of asynchrony of the tautomerization process (for the synchronous processes it equals 0) on the width of the transition state zone of the tautomization reaction (Figure 4).

At the analysis of Table 3 it attracts attention at least five remarkable facts.

First, the A•T↔A*•T* (Brovarets' & Hovorun, 2014b, 2015h) and G·T↔G*·T* (Brovarets' et al., 2015) tautomerization reactions *via* the DPT have an abnormally narrow area of the products of tautomerization (0.58 and 0.99 Bohr, accordingly). The G·C↔G*·C* (0.95) (Brovarets' & Hovorun, 2014e), A•A*↔A*•A (0.62) (Brovarets', Zhurakivsky, & Hovorun, 2013b), G·G*↔G*·G (1.08) (Brovarets' & Hovorun, 2014d), T•T*↔T*•T (0.58) (Brovarets' et al., 2014a), G•G*$_{syn}$↔G*•G*$_{syn}$ (0.97) (Brovarets' & Hovorun, 2014a), H*•T↔H•T* (1.01) (Brovarets' & Hovorun, 2013c; Brovarets' et al., 2013a), H•H↔H*•H* (0.54) (Brovarets' & Hovorun, 2013c; Brovarets', Zhurakivsky, & Hovorun, 2013c), H*•H↔H•H* (0.52 Bohr) (Brovarets' & Hovorun, 2013c; Brovarets' et al., 2013a) have narrow TS region.

Secondly, for 14 out of 21 tautomerization reactions, that is, in 66.7 % of the cases, the transition zone is narrower than the zone of reactant or product of the reaction. Third, in the vast majority of cases, the reagent zone is equal or wider than the zone of the tautomerization product. Fourthly, among the asynchronous processes of the DPT tautomerization the H*•T↔H•T* (Brovarets' & Hovorun, 2013c; Brovarets' et al., 2013a), C·C*↔C*·C (Brovarets' & Hovorun, 2013b), and G•C↔G*•C* (Brovarets' & Hovorun, 2014e) reactions have the lowest degree of asynchrony (0.01, 0.06, and 0.11 Bohr, accordingly), while for the A•A*↔A*•A (Brovarets', Zhurakivsky, & Hovorun, 2013b), T•T*↔T*•T (Brovarets' et al., 2014a), H*•H↔H•H* (Brovarets' & Hovorun, 2013c; Brovarets', Zhurakivsky, & Hovorun, 2013c) tautomerization reactions *via* the DPT this value equals zero. Fifthly, for the synchronous

Table 2. Symmetrical properties of the reagent, product and TS of the tautomerization reactions *via* the DPT in the H-bonded nucleobase pairs obtained at the B3LYP/6–311++G(d,p) level of theory in the free state.

N	Tautomerization reaction *via* the DPT	Nature of the TS	Symmetry of the initial/final complexes	Symmetry of the TS
1	A•T↔A*•T* (Brovarets' & Hovorun, 2014b, 2015h)	Covalently bonded by loosened N6–H–O4 covalent bridge	C_s/C_s	C_s
2	G•C↔G*•C* (Brovarets' & Hovorun, 2014e)	Covalently bonded by loosened O6–H–N4 and N1–H–N3 covalent bridges	C_1/C_1	C_1
3	G·T↔G*·T* (Brovarets' et al., 2015)	Covalently bonded by loosened N1–H–O2 covalent bridge	C_1/C_1	C_1
4	A•A*↔A*•A (Brovarets', Zhurakivsky, & Hovorun, 2013b)	Tight A^+•A^- ion pair	C_s/C_s	C_s
5	A•G↔A*•G* (Brovarets' et al., 2014c)	Covalently bonded by loosened N6–H–N6 covalent bridge	C_1/C_1	C_1
6	G·G*↔G*·G (Brovarets' & Hovorun, 2014d)	Covalently bonded by loosened N1–H–N1 covalent bridge	C_1/C_1	C_1
7	A•C*↔A*·C (Brovarets' & Hovorun, 2015a)	Covalently bonded by loosened N6–H–N4 covalent bridge	C_s/C_s	C_s
8	G*•T↔G•T* (Brovarets', & Hovorun, 2015b, 2015c)	Covalently bonded by loosened N1–H–N3 covalent bridge	C_s/C_s	C_s
9	C·C*↔C*·C (Brovarets' & Hovorun, 2013b)	Tight C^-•C^+ ion pair	C_1/C_1	C_1
10	C•T↔C*•T* (Brovarets' & Hovorun, 2013a)	Covalently bonded by loosened N4–H–O4 covalent bridge	C_1/C_1	C_1
11	T•T*↔T*•T (Brovarets' et al., 2014a)	Symmetrical covalently bonded by loosened O4–H–O4 and N3–H–N3 covalent bridges	C_1/C_1	C_{2v}
12	G•G^*_{syn}↔G^*•G^*_{syn} (Brovarets' & Hovorun, 2014a)	Covalently bonded by loosened O6–H–O6 covalent bridge	C_1/C_1	C_1
13	A*•A_{syn}↔A•A^*_{syn} (Brovarets' et al., 2014b)	Covalently bonded by loosened N1–H–N7 covalent bridge	C_s/C_s	C_1
14	A*•G^*_{syn}↔A•G^*_{syn} (Brovarets' & Hovorun, 2014c)	Covalently bonded by loosened N1–H–N7 covalent bridge	C_s/C_s	C_1
15	H•C↔H*•C* (Brovarets' & Hovorun, 2013c; Brovarets' et al., 2013a)	Tight H^-•C^+ ion pair	C_s/C_s	C_s
16	H*•T↔H•T* (Brovarets' & Hovorun, 2013c; Brovarets' et al., 2013a)	Covalently bonded by loosened N1–H–N3 covalent bridge	C_s/C_s	C_s
17	H•H↔H*•H* (Brovarets' & Hovorun, 2013c; Brovarets' et al., 2013a)	Covalently bonded by loosened O6–H–N1 and N1–H–O6 covalent bridge	C_{2h}/C_{2h}	C_{2h}
18	H*•H↔H•H* (Brovarets' & Hovorun, 2013c; Brovarets', Zhurakivsky, & Hovorun, 2013c)	Symmetrical covalently bonded by loosened O6–H–O6 and N1–H–N1 covalent bridge	C_s/C_s	C_{2v}
19	H·A↔H*·A* (Brovarets' & Hovorun, 2013c; Brovarets' et al., 2014d)	Covalently bonded by loosened O6–H–N6 covalent bridge	C_s/C_s	C_s
20	T·2AP*↔T*·2AP (Brovarets' & Pérez-Sánchez, 2016; Brovarets' et al., 2017a)	Covalently bonded by loosened N3–H–N2 covalent bridge	C_s/C_s	C_s
21	G·2AP*↔G*·2AP (Brovarets' & Pérez-Sánchez, 2016; Brovarets' et al., 2017a)	Covalently bonded by loosened N1–H–N2 covalent bridge	C_1/C_1	C_1

processes of the A•A*↔A*•A (Brovarets', Zhurakivsky, & Hovorun, 2013b), T•T*↔T*•T (Brovarets' et al., 2014a), H*•H↔H•H* (Brovarets' & Hovorun, 2013c; Brovarets', Zhurakivsky, & Hovorun, 2013c) DPT tautomerizations, characterized by a minimum set of KPs, the length of the reagent zone coincides with the length of the reaction product zone. The same regularity is observed only for single synchronous process of the A•A*↔A*•A (Brovarets', Zhurakivsky, & Hovorun, 2013b) DPT tautomerization with nine KPs.

Obtained results allow to make the generalization according the nature of the TS, controlling the course of the DPT reaction, from the point of view of its electronic structure and symmetry (Table 2).

In the vast majority of cases the symmetry of the final, tautomerized complex and TS of tautomerization remain unchanged: C_1 (G·C↔G*·C* (Brovarets' & Hovorun, 2014e), G·T↔G*·T* (Brovarets' et al., 2015), A•G↔A*•G* (Brovarets' et al., 2014c), G·G*↔G*·G (Brovarets' & Hovorun, 2014d), C·C*↔C*·C (Brovarets' & Hovorun, 2013b), C•T↔C*•T* (Brovarets' &

Table 3. Characteristic features of the zones of the reagent, product, and TS of the tautomerization reactions *via* the DPT in the H-bonded nucleobase pairs obtained at the B3LYP/6–311++G(d,p) level of theory in the free state.

N	Tautomerization reaction *via* the DPT	Number of KPs	Type of tautomerization reaction	Width of zone, Bohr			Degree of the asyncrony*, Bohr
				Reactant	TS	Product	
1	A•T↔A*•T* (Brovarets' & Hovorun, 2015h)	9	Asynchronous concerted	4.07	4.15	0.58	3.87
2	G•C↔G*•C* (Brovarets' & Hovorun, 2014e)	9	Asynchronous concerted	7.53	0.95	6.04	0.11
3	G·T↔G*·T* (Brovarets' et al., 2015)	9	Asynchronous concerted	7.22	1.59	0.99	1.23
4	A•A*↔A*•A (Brovarets', Zhurakivsky, & Hovorun, 2013b)	9	Synchronous concerted	2.74	0.62	2.74	0.00
5	A•G↔A*•G* (Brovarets' et al., 2014c)	8	Asynchronous concerted	8.34	3.98	2.62	3.46
6	G·G*↔G*·G (Brovarets' & Hovorun, 2014d)	9	Asynchronous concerted	24.84	1.08	6.56	0.50
7	A•C*↔A*·C (Brovarets' & Hovorun, 2015a)	9	Asynchronous concerted	4.37	1.86	3.69	1.10
8	G*•T↔G•T* (Brovarets', & Hovorun, 2015b, 2015c)	9	Asynchronous concerted	4.06	2.26	3.39	1.68
9	C·C*↔C*·C (Brovarets' & Hovorun, 2013b)	9	Asynchronous concerted	6.91	1.18	6.27	0.06
10	C•T↔C*•T* (Brovarets' & Hovorun, 2013a)	9	Asynchronous concerted	5.86	3.80	3.36	3.12
11	T•T*↔T*•T (Brovarets' et al., 2014a)	5	Synchronous concerted	8.70	0.58	8.70	0.00
12	G•G*$_{syn}$↔G*•G*$_{syn}$ (Brovarets' & Hovorun, 2014a)	8	Asynchronous concerted	8.11	0.97	3.39	0.55
13	A*•A$_{syn}$↔A•A*$_{syn}$ (Brovarets' et al., 2014b)	8	Asynchronous concerted	6.61	1.34	3.49	0.84
14	A*•G*$_{syn}$↔A•G*$_{syn}$ (Brovarets' & Hovorun, 2014c)	9	Asynchronous concerted	3.27	5.79	3.42	5.17
15	H•C↔H*•C* (Brovarets' & Hovorun, 2013c; Brovarets' et al., 2013a)	9	Asynchronous concerted	4.14	1.45	2.79	0.57
16	H*•T↔H•T* (Brovarets' & Hovorun, 2013c; Brovarets' et al., 2013a)	9	Asynchronous concerted	5.44	1.01	4.31	0.01
17	H•H↔H*•H* (Brovarets' & Hovorun, 2013c; Brovarets' et al., 2013a)	6	Asynchronous concerted	6.30	0.54	3.17	0.14
18	H*•H↔H•H* (Brovarets' & Hovorun, 2013c; Brovarets', Zhurakivsky, & Hovorun, 2013c)	5	Synchronous concerted	5.35	0.52	5.35	0.00
19	H·A↔H*·A* (Brovarets' & Hovorun, 2013c; Brovarets' et al., 2014d)	9	Asynchronous concerted	4.75	3.71	2.08	3.19
20	T·2AP*↔T*·2AP (Brovarets' & Pérez-Sánchez, 2016; Brovarets' et al., 2017a)	9	Asynchronous concerted	3.76	5.27	2.87	4.79
21	G·2AP*↔G*·2AP (Brovarets' & Pérez-Sánchez, 2016; Brovarets' et al., 2017a)	9	Asynchronous concerted	6.02	1.70	6.69	1.18

*This parameter we have defined by the formula ||IRC(KP8)|-| IRC(KP2)||.

Hovorun, 2013a), G•G*$_{syn}$↔G*•G*$_{syn}$ (Brovarets' & Hovorun, 2014a) and G·2AP*↔G*·2AP (Brovarets' & Pérez-Sánchez, 2016; Brovarets' et al., 2017a)), C_s (A•T↔A*•T* (Brovarets' & Hovorun, 2014b, 2015h), A•A*↔A*•A (Brovarets', Zhurakivsky, & Hovorun, 2013b), A•C*↔A*·C (Brovarets' & Hovorun, 2015a), G*•T↔G•T* (Brovarets', & Hovorun, 2015b, 2015c), H•C↔H*•C* (Brovarets' & Hovorun, 2013c; Brovarets' et al., 2013a), H*•T↔H•T* (Brovarets' & Hovorun, 2013c; Brovarets' et al., 2013a), H·A↔H*·A* (Brovarets' & Hovorun, 2013c; Brovarets' et al., 2014d), and T·2AP*↔T*·2AP (Brovarets' & Pérez-Sánchez, 2016; Brovarets' et al., 2017a)) and C_{2h} (H•H↔H*•H* (Brovarets' & Hovorun, 2013c; Brovarets' et al., 2013a)). It was also found two cases, when TS has lower symmetry (C_1), than initial and terminal, tautomerized complex (C_s): A*•A$_{syn}$↔A•A*$_{syn}$ (Brovarets' et al., 2014b) and A*•G*$_{syn}$↔A•G*$_{syn}$ (Brovarets' & Hovorun, 2014c). At the same time, it was registered two cases, when TS has higher symmetry (C_{2v}) than initial and terminal, tautomerized complexes: C_1 (T•T*↔T*•T (Brovarets' et al., 2014a)) and C_s (H•H*↔H*•H (Brovarets' &

Table 4. Electron-topological and structural characteristics of the intermolecular bonds revealed in the nine key points (KPs) and the polarity of the latters along the IRC of the biologically important A•C*↔A*•C tautomerization *via* the DPT obtained at the B3LYP/6–311++G(d,p) level of theory in the free state (see Figs. 7, 8) (Brovarets' & Hovorun, 2015a).

Complex	AH•••B H-bond/A–H/H–B covalent bond	ρ^a	$\Delta\rho^b$	$100{\cdot}\varepsilon^c$	$d_{A\cdots B}{}^d$	$d_{H\cdots B}{}^e$	∠AH•••B^f	μ^g
KP 1 (A•C*)	N6H···N4	0.029	0.082	7.626	2.983	1.959	173.8	3.10
	N3H···N1	0.040	0.093	6.584	2.895	1.852	178.9	
	C2H···O2	0.005	0.017	1.478	3.628	2.798	133.1	
KP 2 ($\Delta\rho_{N1\cdots H} = 0$)	N6H···N4	0.062	0.107	6.245	2.702	1.647	175.2	1.99
	N3H···N1	0.110	0.000	4.165	2.624	1.423	179.9	
	C2H···O2	0.007	0.022	1.696	3.443	2.632	131.0	
KP 3 ($\rho_{N1\text{-}H} = \rho_{H\text{-}N3}$)	N6H···N4	0.064	0.101	6.203	2.698	1.634	175.3	1.79
	N3-H-N1	0.148	−0.190	3.534	2.626	1.310	179.8	
	C2H···O2	0.007	0.022	1.444	3.444	2.630	131.2	
KP 4 ($\Delta\rho_{H\cdots N3} = 0$)	N6H···N4	0.068	0.093	6.117	2.690	1.612	175.6	2.51
	N1H···N3	0.106	0.000	4.960	2.637	1.446	179.3	
	C2H···O2	0.007	0.022	1.269	3.449	2.633	131.5	
KP 5 ($\Delta\rho_{H\cdots N4} = 0$)	N6H···N4	0.111	0.000	4.982	2.597	1.419	177.9	2.24
	N1H···N3	0.076	0.077	5.737	2.675	1.574	177.9	
	C2H···O2	0.007	0.021	1.674	3.484	2.671	131.3	
KP 6 ($TS_{A\cdot C^*\leftrightarrow A^*\cdot C}$)	N1H···N3	0.075	0.082	5.782	2.677	1.582	177.9	2.01
	C2H···O2	0.007	0.021	1.677	3.484	2.671	131.3	
KP 7 ($\rho_{N6\text{-}H} = \rho_{H\text{-}N4}$)	N6-H-N4	0.151	−0.202	4.016	2.590	1.294	177.9	1.81
	N1H···N3	0.072	0.089	5.843	2.679	1.594	177.8	
	C2H···O2	0.007	0.021	1.681	3.484	2.672	131.2	
KP 8 ($\Delta\rho_{N6\cdots H} = 0$)	N4H···N6	0.113	0.000	4.645	2.589	1.405	177.8	2.32
	N1H···N3	0.069	0.098	5.913	2.681	1.608	177.8	
	C2H···O2	0.007	0.021	1.688	3.485	2.674	131.1	
KP 9 (A*•C)	N4H···N6	0.037	0.092	7.133	2.905	1.866	176.2	3.83
	N1H···N3	0.040	0.097	6.874	2.871	1.832	180.0	
	C2H···O2	0.005	0.017	2.163	3.583	2.763	132.2	

[a]The electron density at the (3,-1) BCP, a.u.
[b]The Laplacian of the electron density at the (3,-1) BCP, a.u.
[c]The ellipticity at the (3,-1) BCP.
[d]The distance between A (H-bond donor) and B (H-bond acceptor) atoms of the AH···B H-bond, Å.
[e]The distance between H and B atoms of the AH···B H-bond, Å.

Hovorun, 2013c; Brovarets', Zhurakivsky, & Hovorun, 2013c)).

In the vast majority of cases TSs represent themselves structures stabilized by one ($TS_{A\cdot T\leftrightarrow A^*\cdot T^*}$, $TS_{G\cdot T\leftrightarrow G^*\cdot T^*}$, $TS_{A\cdot G\leftrightarrow A^*\cdot G^*}$, $TS_{G\cdot G^*\leftrightarrow G^*\cdot G}$, $TS_{A\cdot C^*\leftrightarrow A^*\cdot C}$, $TS_{G^*\cdot T\leftrightarrow G\cdot T^*}$, $TS_{C\cdot T\leftrightarrow C^*\cdot T^*}$, $TS_{G\cdot G^*syn\leftrightarrow G^*\cdot G^*syn}$, $TS_{A^*\cdot A\text{-}syn\leftrightarrow A\cdot A^*syn}$, $TS_{A^*\cdot G^*syn\leftrightarrow A\cdot G^*syn}$, $TS_{H^*\cdot T\leftrightarrow H\cdot T^*}$, $TS_{H\cdot A\leftrightarrow H^*\cdot A^*}$, $TS_{T\cdot 2AP^*\leftrightarrow T^*\cdot 2AP}$, $TS_{G\cdot 2AP^*\leftrightarrow G^*\cdot 2AP}$) or two ($TS_{G\cdot C\leftrightarrow G^*\cdot C^*}$, $TS_{T\cdot T^*\leftrightarrow T^*\cdot T}$, $TS_{H\cdot H\leftrightarrow H^*\cdot H^*}$, $TS_{H^*\cdot H\leftrightarrow H\cdot H^*}$) loosened A–H–B covalent bridges. In the cases of the $TS_{T\cdot T^*\leftrightarrow T^*\cdot T}$, $TS_{G\cdot G^*syn\leftrightarrow G^*\cdot G^*syn}$, $TS_{A^*\cdot Asy\text{-}n\leftrightarrow A\cdot A^*syn}$, $TS_{H\cdot A\leftrightarrow H^*\cdot A^*}$, and $TS_{H^*\cdot H\leftrightarrow H\cdot H^*}$ these bridges are symmetrical. It was fixed three cases of tautomerization – A•A*↔A*•A (Brovarets', Zhurakivsky, & Hovorun, 2013b), C•C*↔C*•C (Brovarets' & Hovorun, 2013b), H•C↔H*•C* (Brovarets' & Hovorun, 2013c; Brovarets' et al., 2013a) – controlled by the TSs, which are asymmetric tight ion pairs $A^+{\cdot}A^-$, $C^-{\cdot}C^+$, and $H^-{\cdot}C^+$, with the quite high energy of stabilization exceeding 100 kcal•mol^{-1} (Figure 1, Table 2).

This methodology of the sweeps of the physicochemical parameters enables us to obtain the profiles of the intermolecular interactions (AH···B H-bonds, in particular non-classical CH···O/N (Brovarets', Yurenko, & Hovorun, 2013, 2015), loosened A–H–B covalent bridges and attractive A···B van der Waals contacts (Matta & Boyd, 2007)) along the IRC.

Based on these data (Figure 5), we have obtained interesting regularities and generalizations.

This methodology enables to make an objective conclusion about the character of the tautomerization (concerted, synchronous, or asynchronous), quantitatively estimate the cooperativity of the specific intermolecular interactions (AH···B H-bonds, in particular non-classical CH···O/N, loosened A–H–B covalent bridges, and attractive A···B van der Waals contacts), sequentially changing each other along the IRC of tautomerization, and trace how these interactions are grouped into the patterns (three and five) and how they consistently substitute each other along the IRC of tautomerization. Energy of the intermolecular specific contacts (in particular, H-bonds or

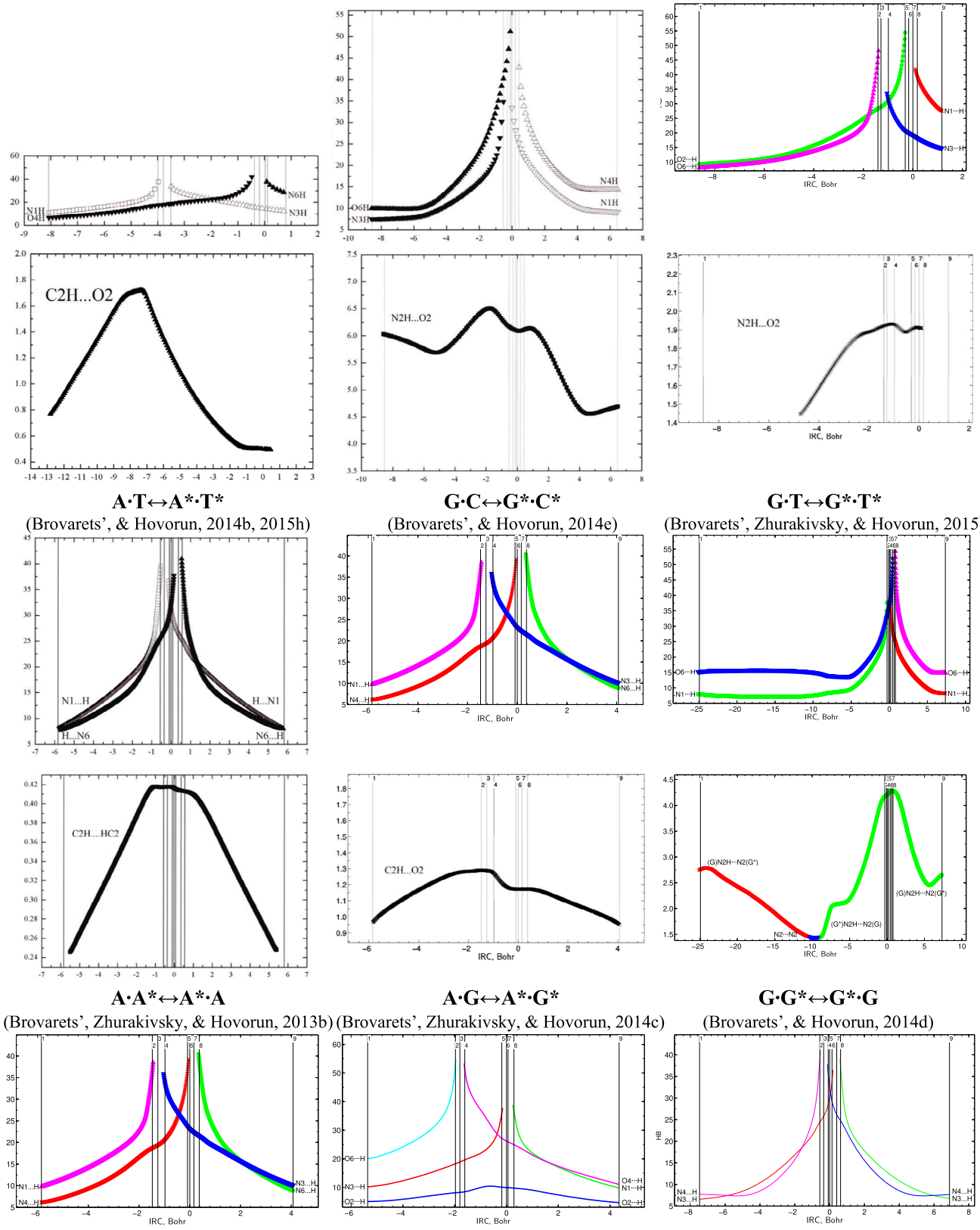

Figure 5. Profiles of the energy of the intermolecular H-bonds or van der Waals contacts estimated by the EML formula at the (3,-1) BCPs (Espinosa et al., 1998; Mata et al., 2011; Matta et al., 2006) along the IRC of the tautomerization reactions *via* the DPT obtained at the B3LYP/6–311++G(d,p) level of theory in the free state.

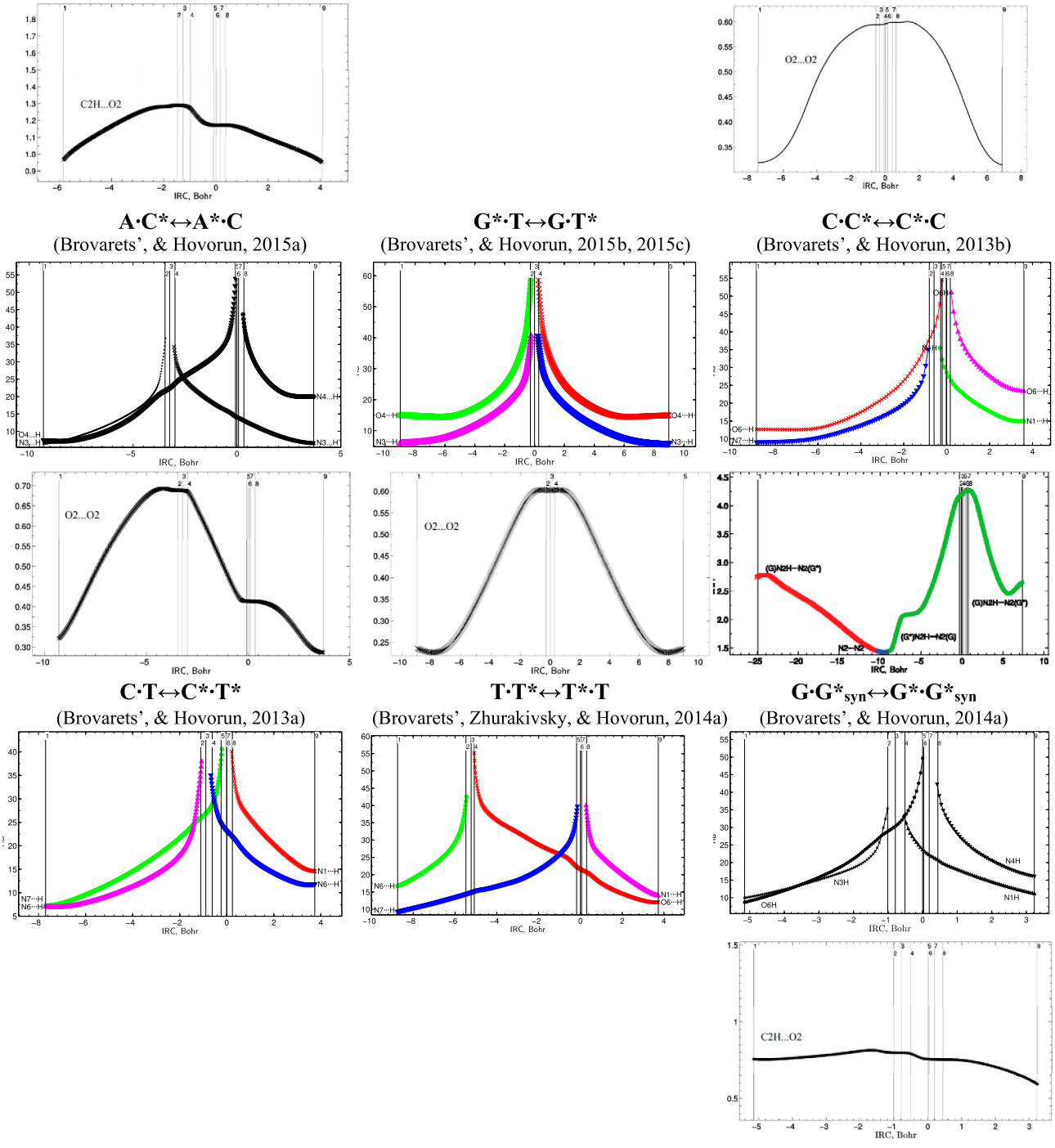

A·C*↔A*·C
(Brovarets', & Hovorun, 2015a)

G*·T↔G·T*
(Brovarets', & Hovorun, 2015b, 2015c)

C·C*↔C*·C
(Brovarets', & Hovorun, 2013b)

C·T↔C*·T*
(Brovarets', & Hovorun, 2013a)

T·T*↔T*·T
(Brovarets', Zhurakivsky, & Hovorun, 2014a)

G·G*$_{syn}$↔G*·G*$_{syn}$
(Brovarets', & Hovorun, 2014a)

A*·A$_{syn}$↔A·A*$_{syn}$
(Brovarets', Zhurakivsky, & Hovorun, 2014b)

A*·G*$_{syn}$↔A·G*$_{syn}$
(Brovarets', & Hovorun, 2014c)

H·C↔H*·C*
(Brovarets', & Hovorun, 2013c; Brovarets', Zhurakivsky, & Hovorun, 2013a)

Figure 5. (*Continued*)

van der Waals contacts) has been calculated by the Espinosa–Molins–Lecomte formula (Espinosa, Molins, & Lecomte, 1998; Mata, Alkorta, Espinosa, & Molins, 2011), which has been firstly applied for the DNA dimers by Prof. Matta *et al.* (Matta, Castillo, & Boyd, 2006).

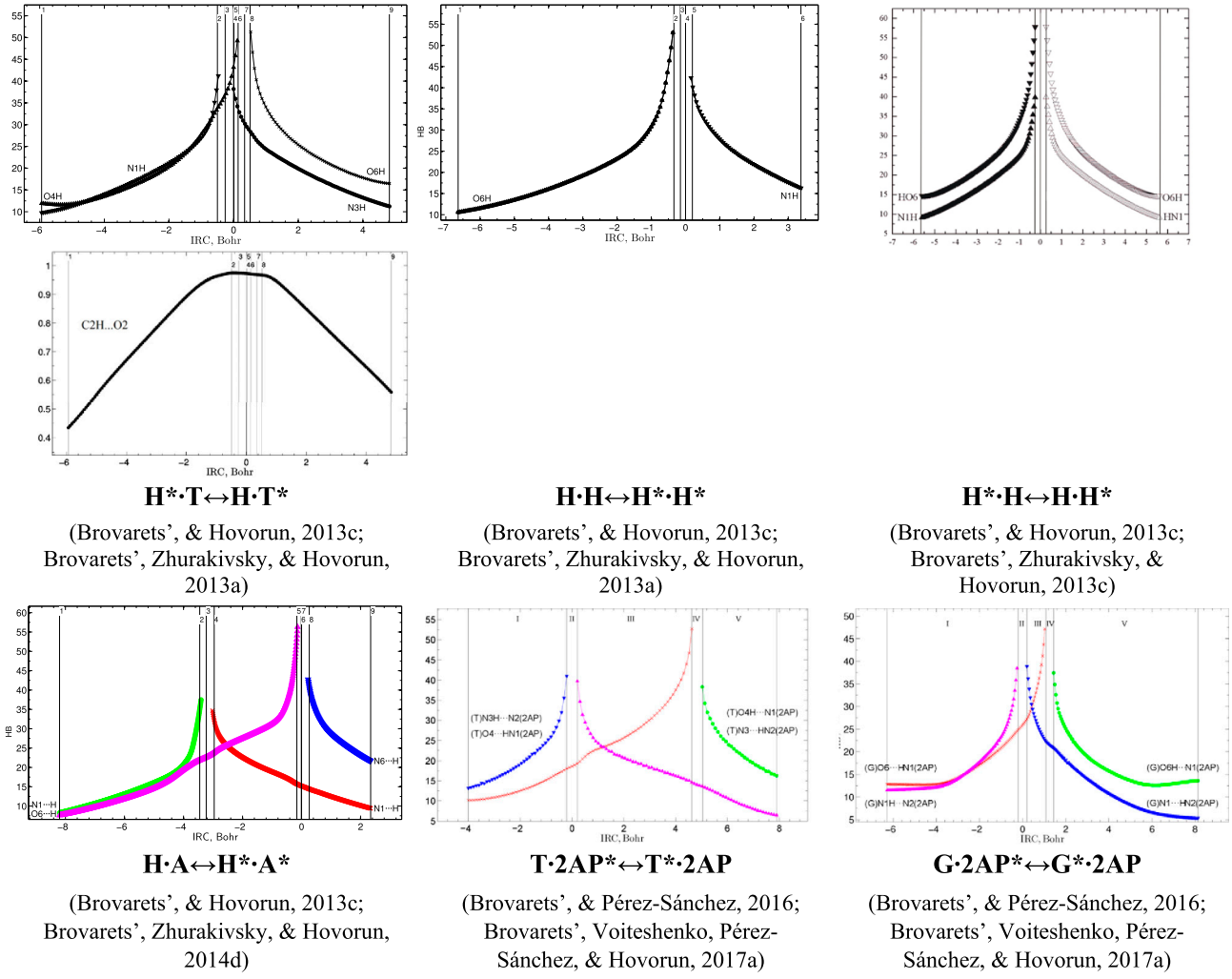

H*·T↔H·T*

(Brovarets', & Hovorun, 2013c; Brovarets', Zhurakivsky, & Hovorun, 2013a)

H·H↔H*·H*

(Brovarets', & Hovorun, 2013c; Brovarets', Zhurakivsky, & Hovorun, 2013a)

H*·H↔H·H*

(Brovarets', & Hovorun, 2013c; Brovarets', Zhurakivsky, & Hovorun, 2013c)

H·A↔H*·A*

(Brovarets', & Hovorun, 2013c; Brovarets', Zhurakivsky, & Hovorun, 2014d)

T·2AP*↔T*·2AP

(Brovarets', & Pérez-Sánchez, 2016; Brovarets', Voiteshenko, Pérez-Sánchez, & Hovorun, 2017a)

G·2AP*↔G*·2AP

(Brovarets', & Pérez-Sánchez, 2016; Brovarets', Voiteshenko, Pérez-Sánchez, & Hovorun, 2017a)

Figure 5. (*Continued*)

First, these interactions could be grouped into the specific patterns, that sequentially change each other along the IRC of tautomerization (Brovarets', 2010, 2015; Brovarets' & Hovorun, 2013a, 2013b, 2013c, 2014a, 2014b, 2014c, 2014d, 2014e, 2015a, 2015b, 2015c, 2015d, 2015e, 2015f, 2015g, 2015h; Brovarets' et al., 2013a, 2013b, 2013c, 2014a, 2014b, 2014c, 2014d, 2015; Brovarets' & Pérez-Sánchez, 2016, 2017; Brovarets', Pérez-Sánchez, et al., 2016; Brovarets', Voiteshenko, et al., 2018; Brovarets', Voiteshenko, Pérez-Sánchez, et al., 2017a, 2018) (Figure 5). It was revealed three such patterns for the synchronous DPT tautomerization, while five – for the asynchronous (Figures 1, 5, Table 1, 2). Secondly, neighboring antiparallel H-bonds strengthen each other; in those cases, when neighboring H-bonds become parallel, they cooperatively weaken each other (Figures 1, 5). Using the profiles of the energies of the H-bonds on IRC, it is easy to quantitively estimate their cooperative or anti-cooperative properties.

In those cases, when tautomerization of the complexes does not occur, as it takes place in the G·A_{syn} DNA base mispair (Brovarets' & Hovorun, 2014c), we have developed quite simple methodology for the estimation of the interdependence of the neighboring H-bonds, that are involved in the stabilization of these complexes. It consists in the forced stretching of the N6H and N1H atomic groups – donors of the N6H···O6 and N1H···N7 H-bonds in the G·A_{syn} DNA base mispair, respectively, with further sequential fixation of their length and geometry optimization (Figure 6). As a result, we found out, that the neighboring N6H···O6 and N1H···N7 H-bonds are cooperative, strengthening each other (Figure 6).

Thirdly, it was established that the DPT processes are assisted by the third specific intermolecular contact – H-bond or attractive van der Waals contact, exposed into the DNA minor groove, except the cases of the A*•A_{syn}↔A•A*$_{syn}$ (Brovarets' et al., 2014b), A*•G*$_{syn}$↔A•G*-$_{syn}$ (Brovarets' & Hovorun, 2014c), H•H↔H*•H*

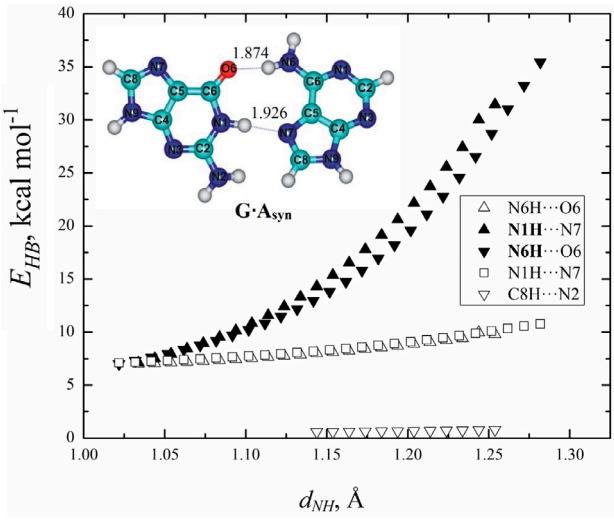

Figure 6. Graphs of the energy of the H-bonds E_{HB}, estimated by the EML formula (Espinosa et al., 1998; Mata et al., 2011; Matta et al., 2006), at the (3,-1) BCPs of the H-bonds in the G•A$_{syn}$ DNA base mispair, as a function of the distance d_{NH} obtained at the B3LYP/6–311++G(d,p) level of theory in the free state. The forcibly changed distances $d_{N1H/N6H}$ are shown in bold (Brovarets' & Hovorun, 2014c).

(Brovarets' & Hovorun, 2013c; Brovarets' et al., 2013a), H*•H↔H•H* (Brovarets' & Hovorun, 2013c; Brovarets', Zhurakivsky, & Hovorun, 2013c), H·A↔H*·A* (Brovarets' & Hovorun, 2013c; Brovarets' et al., 2014d), T·2AP*↔T*·2AP (Brovarets' & Pérez-Sánchez, 2016; Brovarets' et al., 2017a), and G·2AP*↔G*·2AP (Brovarets' & Pérez-Sánchez, 2016; Brovarets' et al., 2017a) tautomerization reactions (Figures 1, 5). Fourthly and lastly, graphs of the ellipticities of the H-bonds or attractive van der Waals contacts demonstrate the appearance or disappearance in a certain range of the IRC tautomerization. In those cases, when these specific intermolecular interactions switch, that is transform one into the other, ellipticity ε does not show any anomalies (Figures 8(c) and 9). Conversely, when specific intermolecular interactions are included or excluded, then at approaching to these points, their ellipticity sharply increases (Figure 9), that points on the dynamical non-stability of their interactions.

Transition from vacuum into the low polar continuum with ε = 4, characteristic for the hydrophobic interfaces of the protein–DNA complexes (Mertz & Krishtalik, 2000; Petrushka, Sowers, & Goodman, 1986), does not significantly influence the course of these tautomerization reactions and does not change the character of the obtained conlcusions and generalizations.

It draws the attention that in the course of the aforementioned reactions the heterocycles of the nucleotide bases hold their planarity, despite their ability to bend quite easily (Govorun et al., 1992; Hovorun, Gorb, & Leszczynski, 1999; Nikolaienko, Bulavin, & Hovorun, 2011), and the methyl group of the T DNA base does not change its orientation.

The other, purely technical and methodological conclusion concerns the used B3LYP/6–311++G(d,p) level

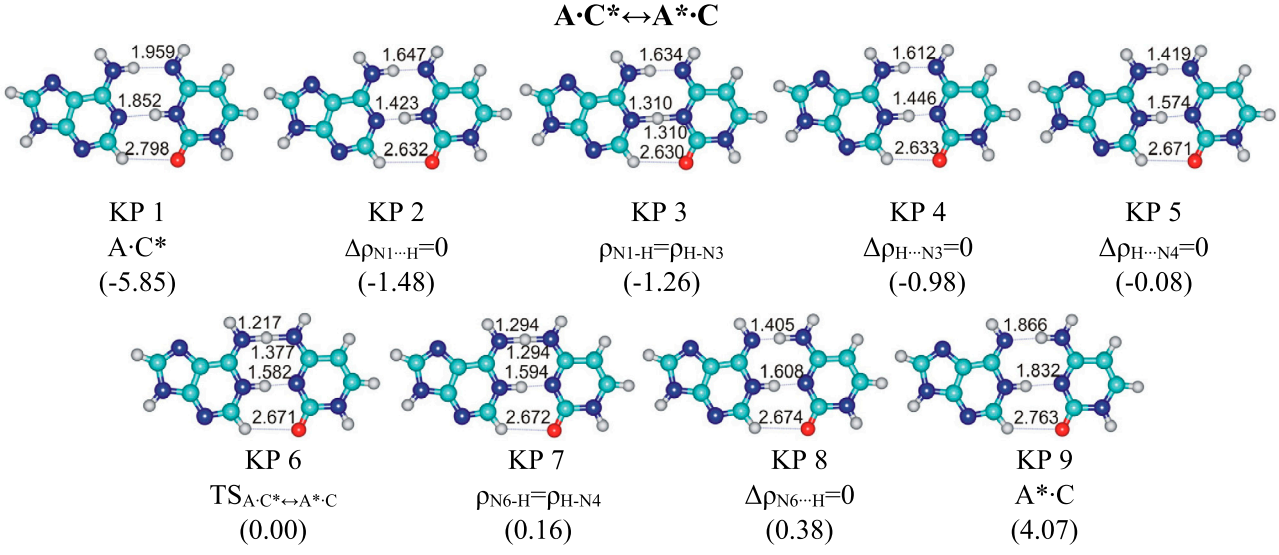

Figure 7. Geometric structures of the nine key points (KPs) describing the evolution of the biologically important A•C*↔A*•C tautomerization *via* the DPT along the IRC obtained at the B3LYP/6–311++G(d,p) level of theory in the free state (Brovarets' & Hovorun, 2015a). Coordinates of the KPs (in Bohr) are presented below them in brackets. The dotted lines indicate AH···B H-bonds, while continuous lines show covalent bonds (their lengths are presented in angstroms). Carbon atoms are in light blue, nitrogen in dark blue, hydrogen in gray, and oxygen in red.

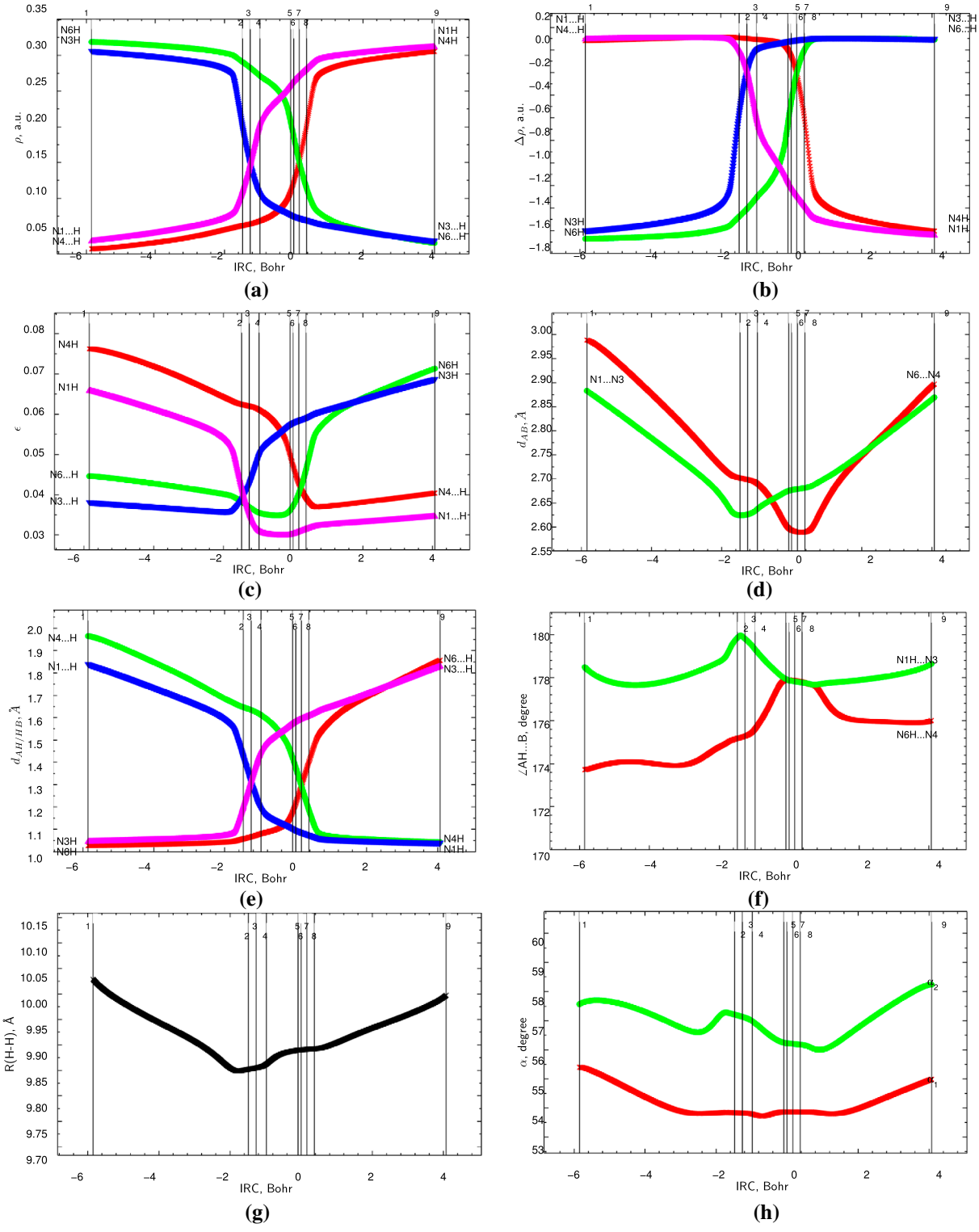

Figure 8. Profiles of: (**a**) the electron density ρ; (**b**) the Laplacian of the electron density Δρ, (**c**) the ellipticity ε at the (3,-1) BCPs, (**d**) the distance $d_{A\cdots B}$ between the electronegative A and B atoms; (**e**) the distance $d_{AH/HB}$ between the hydrogen and electronegative A or B atoms, (**f**) the angle ∠AH···B of the covalent and hydrogen bonds, **(g)** the distance $R(H_1–H_9)$ between the H_1 and H_9 glycosidic hydrogens and **(h)** the α_1 (∠N9HH) and α_2 (∠N1HH) glycosidic angles along the IRC of the biologically important A•C*↔A*•C tautomerization *via* the DPT obtained at the B3LYP/6–311++G(d,p) level of theory in the free state (Brovarets' & Hovorun, 2015a).

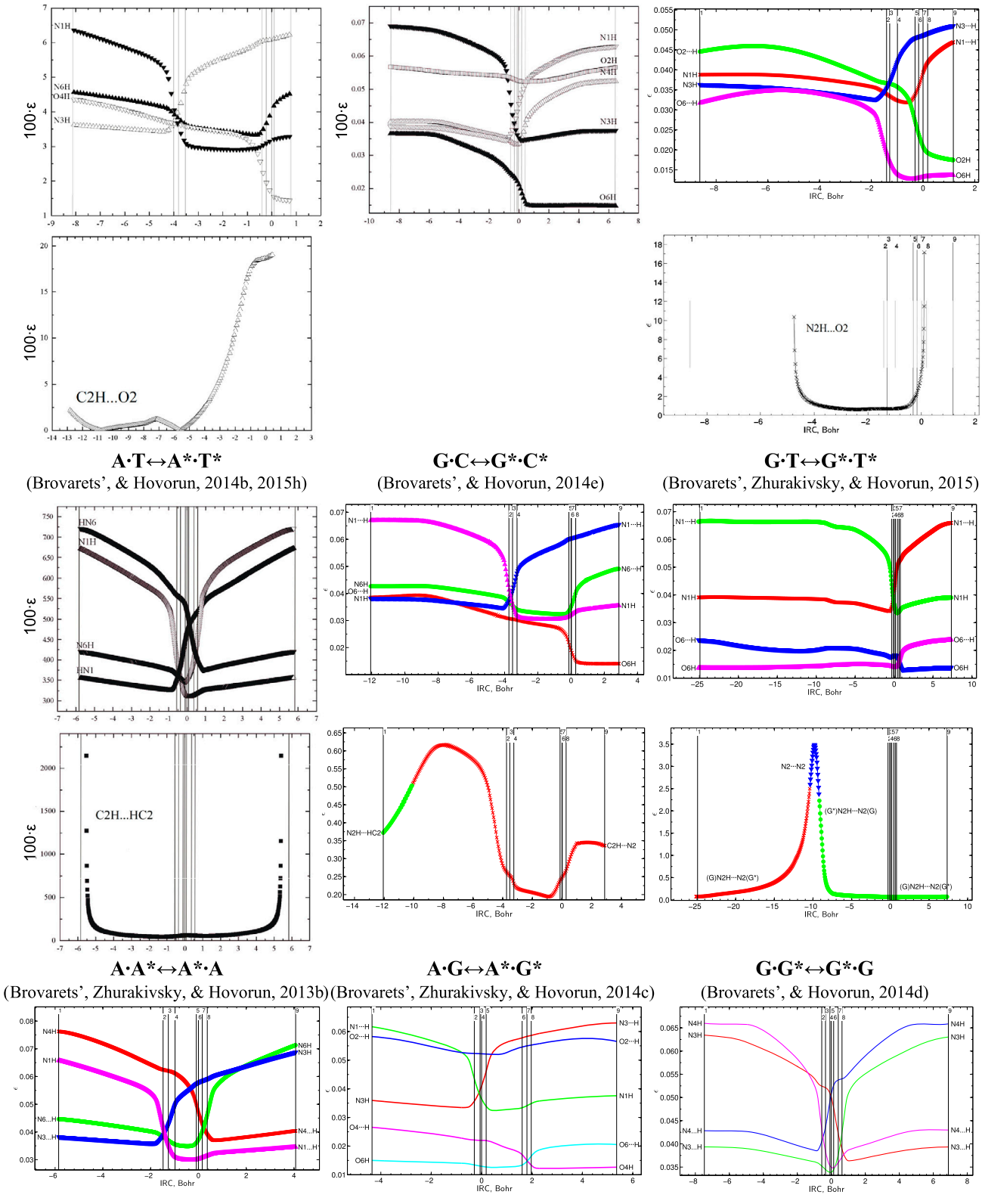

A·T↔A*·T* (Brovarets', & Hovorun, 2014b, 2015h)

G·C↔G*·C* (Brovarets', & Hovorun, 2014e)

G·T↔G*·T* (Brovarets', Zhurakivsky, & Hovorun, 2015)

A·A*↔A*·A (Brovarets', Zhurakivsky, & Hovorun, 2013b)

A·G↔A*·G* (Brovarets', Zhurakivsky, & Hovorun, 2014c)

G·G*↔G*·G (Brovarets', & Hovorun, 2014d)

Figure 9. Profiles of the ellipticity ε of the intermolecular H-bonds and attractive van der Waals contacts at the (3,-1) BCPs along the IRC of the tautomerization reactions *via* the DPT obtained at the B3LYP/6–311++G(d,p) level of theory in the free state. All key points as vertical lines are presented for each profile.

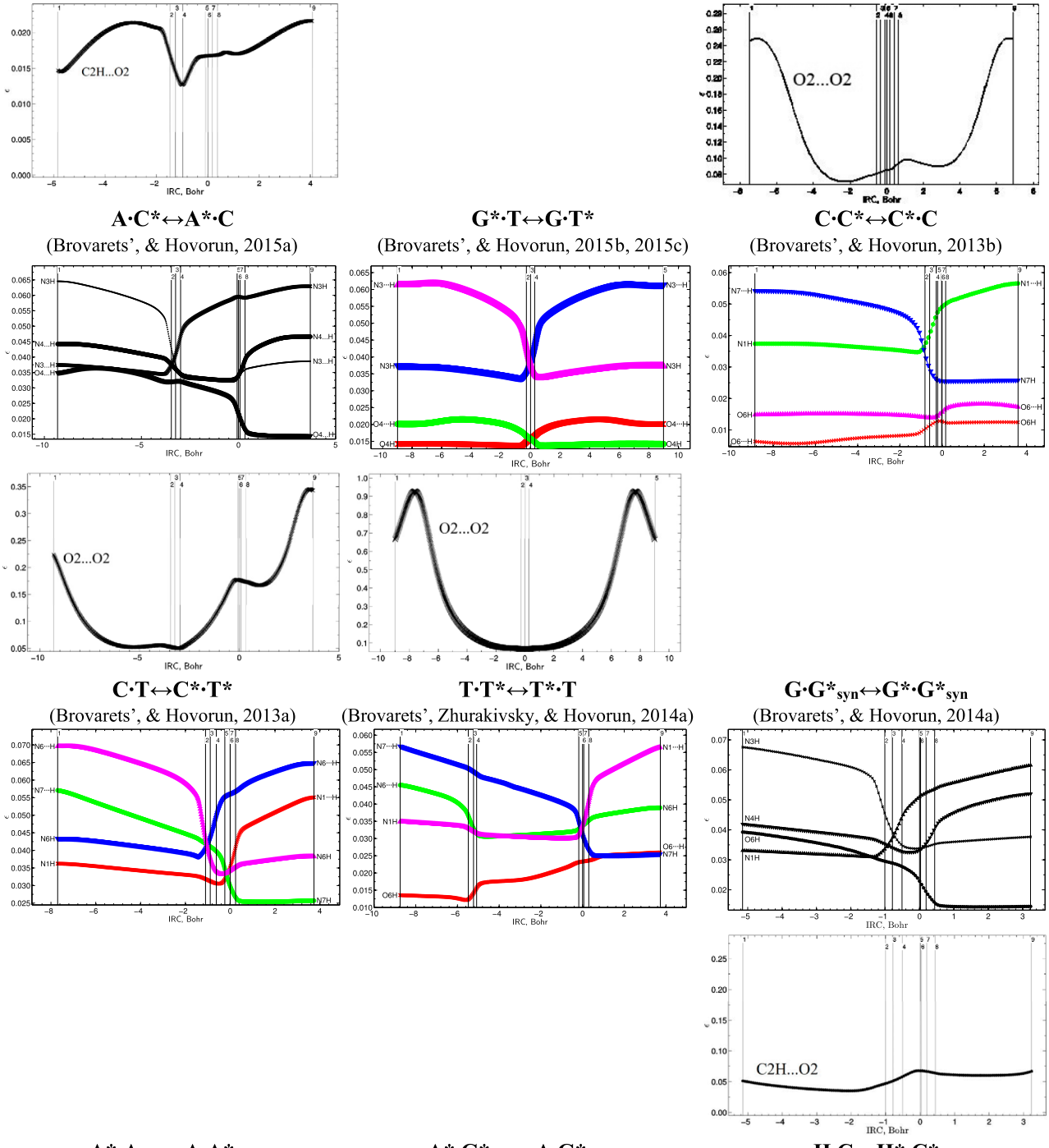

Figure 9. (*Continued*)

of QM theory. Comparison of the results obtained at this level with similar data obtained at the MP2/6–311++G(d, p) level of theory (Brovarets' & Hovorun, 2014b, 2014e, 2015a, 2015c) indicates that the first of them is adequate and moreover represents itself the shortest way to MP2 results (Danilov, Anisimov, Kurita, & Hovorun, 2005;

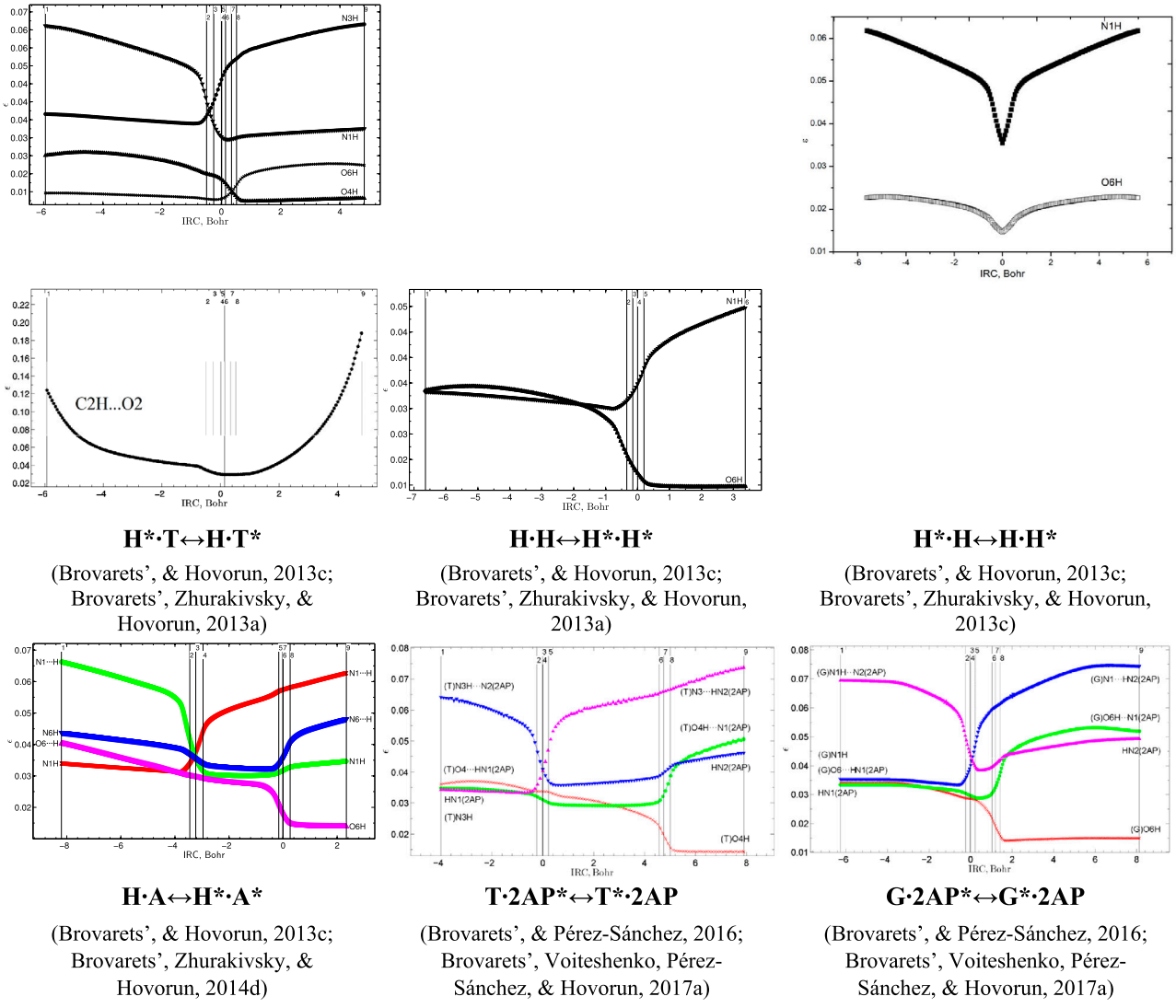

H*·T↔H·T*

(Brovarets', & Hovorun, 2013c; Brovarets', Zhurakivsky, & Hovorun, 2013a)

H·H↔H*·H*

(Brovarets', & Hovorun, 2013c; Brovarets', Zhurakivsky, & Hovorun, 2013a)

H*·H↔H·H*

(Brovarets', & Hovorun, 2013c; Brovarets', Zhurakivsky, & Hovorun, 2013c)

H·A↔H*·A*

(Brovarets', & Hovorun, 2013c; Brovarets', Zhurakivsky, & Hovorun, 2014d)

T·2AP*↔T*·2AP

(Brovarets', & Pérez-Sánchez, 2016; Brovarets', Voiteshenko, Pérez-Sánchez, & Hovorun, 2017a)

G·2AP*↔G*·2AP

(Brovarets', & Pérez-Sánchez, 2016; Brovarets', Voiteshenko, Pérez-Sánchez, & Hovorun, 2017a)

Figure 9. (*Continued*)

Lozynski, Rusinska-Roszak, & Mack, 1998; Matta, 2010).

Finally, we would like to note that proposed by us approaches to the analysis of the atomistic mechanisms are already successfully applied by other authors (Inostroza-Rivera et al., 2015). We hope that they will be intensively used in the future as for the research purposes, in particular at the studying of the mechanisms of the tautomerization of the H-bonded complexes of any kind and structure (Jin et al., 2017, 2018; Palafox & Rastogi, 2016; Shi, Jiang, Zhang, & Wang, 2017; Tolosa et al., 2017, 2018; Yang et al., 2017; Yepes et al., 2013a, 2013b), so in the teaching practice.

It would become clear in the process of the accumulation and generalization of the results of the investigation, whether the H-bonded pairs of nucleotide bases are similar or different from the other H-bonded complexes.

Conclusions

Obtained generalizations enable us to arrive to at least four important conclusions.

(1) Elaborated and implemented into the scientific practice our new conception based on the sweeps of the physicochemical parameters, such as electronic energy E, the first derivative of the electronic energy by the IRC – dE/dIRC, the dipole moment of the base pair μ, the distances $d_{A\cdots B}$, $d_{AH/HB}$, and the angle ∠AH···B of the intermolecular H-bonds, the electron density ρ, the Laplacian of the electron density Δρ, ellipticity ε, and the energy E_{HB} at the (3,-1) bond critical points of the intrapair H-bonds, the NBO charges q_{NBO} of the hydrogen atoms involved in the tau-

tomerization, the glycosidic angles α_1/α_2, and the distance $R(H_{1/9}–H_{1/9})$ between the glycosidic hydrogens, along the entire internal reaction coordinate, and also KPs, that are distinguished on the way of the proton migration along the intermolecular H-bonds, allows to understand the deep essence of the tautomerization processes *via* the DPT. Except scientific, this approach has also pedagogical meaning, in particular it could be applied in the scientific practice at the investigation of the mechanisms of tautomerization of the H-bonded complexes of any origin and structure. Generalized conclusion on the nature of the extrema of the first derivative of the electron energy of the complex by the IRC of its tautomerization – dE/dIRC – considerably extends the scope of the effective application of this function, in particular, in physical chemistry and molecular physics at the investigation of proton mobility processes.

(2) Tautomerization reaction *via* the DPT can be considered successful in those and only in those case if the tautomerized complex is a dynamically stable system, during the lifetime of which low-frequency intermolecular vibrations could develop. Exactly the dynamic stability of the tautomerized pairs is the key to their spontaneous dissociation into the monomers with changed tautomeric status.

(3) It is possible to speak about the mutagenic tautomerization of certain pairs of nucleotide bases only in that case, when the lifetime of the tautomerized base pairs exceeds the time spent by the DNA replication machinery on their forced dissociation (~10^{-9} s). In the opposite case short-lived tautomers of the nucleotide bases pretending on the role of the mutagenic would simply "slip out from the hands" of the DNA replication machinery.

(4) An urgent task for the future is to take into account the quantum tunneling effects in the symmetric complexes, that tautomerize (Brovarets' & Hovorun, 2015h) – A•A*↔A*•A (Brovarets', Zhurakivsky, & Hovorun, 2013b), G•G*↔G*•G (Brovarets' & Hovorun, 2014d), T•T*↔T*•T (Brovarets' et al., 2014a), C•C*↔C*•C (Brovarets' & Hovorun, 2013b), and H•H*↔H*•H (Brovarets' & Hovorun, 2013c; Brovarets', Zhurakivsky, & Hovorun, 2013c). Tunneling is principally impossible for the other cases of tautomerization analyzed in this Review (Brovarets' & Hovorun, 2015h).

Acknowledgments

The authors gratefully appreciate technical support and computational facilities of joint computer cluster of SSI "Institute for Single Crystals" of the National Academy of Sciences of Ukraine (NASU) and Institute for Scintillation Materials of the NASU incorporated into Ukrainian National Grid. This work was partially supported by the Grant of the NASU for young scientists, Grant of the President of Ukraine to support the research of young scientists [project number F70] from the State Fund for Fundamental Research of Ukraine of the Ministry of the Education and Science of Ukraine and by the Scholarship of Verkhovna Rada (Parliament) of Ukraine for the talented young scientists in 2017 year given to DrSci Ol'ha Brovarets'. O. O. B. expresses sincere gratitude to organizing committee for financial support of the participation in the "EMBO/FEBS Lecture Course Spetsai Summer School 2017 for Proteins and Organized Complexity" (September 24–October 1, 2017, Spetses, Greece), to Lawyers Association "AVER Lex" (Kyiv, Ukraine) for the sponsorship of the presenting the plenary lecture as invited speaker at the "EMN Meeting on Computation and Theory" (November 6–10, 2017, Dubai, United Arab Emirates) and to Max Plank Institute of Plant Physiology (hosted by Prof. Yariv Brotman) for the kind invitation and financial support of the invited lecture (November 29, 2017, Potsdam, Germany).

Disclosure statement

No potential conflict of interest was reported by the authors.

ORCID

Ol'ha O. Brovarets' http://orcid.org/0000-0002-8929-293X
Dmytro M. Hovorun http://orcid.org/0000-0002-5579-5520

References

Arabi, A., & Matta, C. F. (2011). Effects of external electric fields on double proton transfer kinetics in the formic acid dimer. *Physical Chemistry Chemical Physics, 13*, 13738–13748. doi:10.1039/c1cp20175a

Atkins, P. W. (1998). *Physical chemistry*. Oxford: Oxford University Press.

Bader, R. F. W. (1990). *Atoms in molecules: A quantum theory*. Oxford: Oxford University Press.

Bebenek, K., Pedersen, L. C., & Kunkel, T. A. (2011). Replication infidelity *via* a mismatch with Watson−Crick geometry. *Proceeding of the National Academy of Sciences of the United States of America, 108*, 1862–1867. doi:10.1073/pnas.1012825108

Bell, R. P. (1973). *The proton in chemistry*. London: Chapman and Hall.

Bell, R. P. (1980). *The tunnel effect in chemistry*. London: Chapman and Hall.

Boutis, T. (1992). *Proton transfer in hydrogen bonded systems*. New York, NY: Plenum.

Brovarets', O. O. (2015). *Microstructural mechanisms of the origin of the spontaneous point mutations* (DrSci Thesis). Taras Shevchenko National University of Kyiv, Kyiv.

Brovarets', O. O. (2010). *Physico-chemical nature of the spontaneous and induced by the mutagens transitions and*

transversions (PhD Thesis). Taras Shevchenko National University of Kyiv, Kyiv.

Brovarets', O. O., & Hovorun, D. M. (2013a). Atomistic understanding of the C·T mismatched DNA base pair tautomerization *via* the DPT: QM and QTAIM computational approaches. *Journal of Computational Chemistry, 34*, 2577–2590. doi:10.1002/jcc.23412

Brovarets', O. O., & Hovorun, D. M. (2013b). Atomistic nature of the DPT tautomerisation of the biologically important C·C* DNA base mispair containing amino and imino tautomers of cytosine: A QM and QTAIM approach. *Physical Chemistry Chemical Physics, 15*, 20091–20104. doi:10.1039/c3cp52644e

Brovarets' O. O., & Hovorun D. M. (2013c). Prototropic tautomerism and basic molecular principles of hypoxanthine mutagenicity: An exhaustive quantum-chemical analysis. *Journal of Biomolecular Structure and Dynamics, 31*, 913–936. doi:10.1080/07391102.2012.715041

Brovarets', O. O., & Hovorun, D. M. (2014a). Does the G·G*$_{syn}$ DNA mismatch containing canonical and rare tautomers of the guanine tautomerise through the DPT? A QM/QTAIM microstructural study. *Molecular Physics, 112*, 3033–3046. doi:10.1080/00268976.2014.927079

Brovarets', O. O., & Hovorun, D. M. (2014b). Can tautomerisation of the A•T Watson-Crick base pair *via* double proton transfer provoke point mutations during DNA replication? A comprehensive QM and QTAIM analysis. *Journal of Biomolecular Structure and Dynamics, 32*, 127–154. doi:10.1080/07391102.2012.755795

Brovarets', O. O., & Hovorun, D. M. (2014c). DPT tautomerisation of the G·A$_{syn}$ and A*·G*$_{syn}$ DNA mismatches: A QM/QTAIM combined atomistic investigation. *Physical Chemistry Chemical Physics, 16*, 9074–9085. doi:10.1039/c4cp00488d

Brovarets', O. O., & Hovorun, D. M. (2014d). How does the long G·G* Watson-Crick DNA base mispair comprising keto and enol tautomers of the guanine tautomerise? The results of a QM/QTAIM investigation. *Physical Chemistry Chemical Physics, 16*, 15886–15899. doi:10.1039/c4cp01241k

Brovarets', O. O., & Hovorun, D. M. (2014e). Why the tautomerization of the G·C Watson-Crick base pair *via* the DPT does not cause point mutations during DNA replication? QM and QTAIM comprehensive analysis. *Journal of Biomolecular Structure & Dynamics, 32*, 1474–1499. doi:10.1080/07391102.2013.822829

Brovarets', O. O., & Hovorun, D. M. (2015a). The physicochemical essence of the purine·pyrimidine transition mismatches with Watson-Crick geometry in DNA: A·C* *versa* A*·C. A QM and QTAIM atomistic understanding. *Journal of Biomolecular Structure & Dynamics, 33*, 28–55. doi:10.1080/07391102.2013.852133

Brovarets', O. O., & Hovorun, D. M. (2015b). How many tautomerisation pathways connect Watson-Crick-like G*·T DNA base mispair and wobble mismatches? *Journal of Biomolecular Structure & Dynamics, 33*, 2297–2315. doi:10.1080/07391102.2015.1046936

Brovarets', O. O., & Hovorun, D. M. (2015c). The nature of the transition mismatches with Watson-Crick architecture: The G*·T or G·T* DNA base mispair or both? A QM/QTAIM perspective for the biological problem. *Journal of Biomolecular Structure & Dynamics, 33*, 925–945. doi:10.1080/07391102.2014.924879

Brovarets', O. O., & Hovorun, D. M. (2015d). Tautomeric transition between wobble A·C DNA base mispair and Watson–Crick-like A·C* mismatch: Microstructural mechanism and biological significance. *Physical Chemistry Chemical Physics, 17*, 15103–15110. doi:10.1039/c5cp01568e

Brovarets', O. O., & Hovorun, D. M. (2015e). A novel conception for spontaneous transversions caused by homo-pyrimidine DNA mismatches: A QM/QTAIM highlight. *Physical Chemistry Chemical Physics, 17*, 21381–21388. doi:10.1039/c5cp03211c

Brovarets', O. O., & Hovorun, D. M. (2015f). Novel physicochemical mechanism of the mutagenic tautomerisation of the Watson-Crick-like A·G and C·T DNA base mispairs: A quantum-chemical picture. *RSC Advances, 5*, 66318–66333. doi:10.1039/C5RA11773A

Brovarets', O. O., & Hovorun, D. M. (2015g). Wobble↔Watson-Crick tautomeric transitions in the homo-purine DNA mismatches: A key to the intimate mechanisms of the spontaneous transversions. *Journal of Biomolecular Structure & Dynamics, 33*, 2710–2715. doi:10.1080/07391102.2015.1077737

Brovarets', O. O., & Hovorun, D. M. (2015h). Proton tunneling in the A•T Watson-Crick DNA base pair: Myth or reality? *Journal of Biomolecular Structure & Dynamics, 33*, 2716–2720. doi:10.1080/07391102.2015.1092886

Brovarets', O. O., Kolomiets', I. M., & Hovorun, D. M. (2012). Elementary molecular mechanisms of the spontaneous point mutations in DNA: A novel quantum-chemical insight into the classical understanding. In T. Tada (Ed.), *Quantum chemistry – molecules for innovations*. InTech Open. Retrieved from http://www.intechopen.com/books/quantum-chemistry-molecules-for-innovations/elementary-molecular-mechanisms-of-the-spontaneous-point-mutations-in-dna-a-novel-quantum-chemical-i

Brovarets', O. O., & Pérez-Sánchez, H. E. (2016). Whether the amino-imino tautomerism of 2-aminopurine is involved into its mutagenicity? Results of a thorough QM investigation. *RSC Advances, 110*, 108255–108264. doi:10.1039/C6RA24277D

Brovarets', O. O., & Pérez-Sánchez, H. E. (2017). Whether 2-aminopurine induces incorporation errors at the DNA replication? A quantum-mechanical answer on the actual biological issue. *Journal of Biomolecular Structure & Dynamics, 35*, 3398–3411. doi:10.1080/07391102.2016.1253504

Brovarets', O. O., Pérez-Sánchez, H. E., & Hovorun, D. M. (2016). Structural grounds for the 2-aminopurine mutagenicity: A novel insight into the old problem of the replication errors. *RSC Advances, 6*, 99546–99557. doi:10.1039/C6RA17787E

Brovarets', O. O., Voiteshenko, I., & Hovorun, D. M. (2018). Physico-chemical profiles of the wobble↔Watson-Crick G*·2AP(w)↔G·2AP(WC) and A·2AP(w)↔A*·2AP(WC) tautomerisations: A QM/QTAIM comprehensive survey. *Physical Chemistry Chemical Physics, 20*, 623–636. doi:10.1039/c7cp05139e

Brovarets', O. O., Voiteshenko, I., Pérez-Sánchez, H. E., & Hovorun, D. M. (2017a). A QM/QTAIM research under the magnifying glass of the DPT tautomerisation of the wobble mispairs involving 2-aminopurine. *New Journal of Chemistry, 41*, 7232–7243. doi:10.1039/C7NJ00717E

Brovarets', O. O., Voiteshenko, I., Pérez-Sánchez, H. E., & Hovorun, D. M. (2018). A QM/QTAIM detailed look at the Watson-Crick↔wobble tautomeric transformations of the 2-aminopurine·pyrimidine mispairs. *Journal of Biomolecular Structure & Dynamics, 36*, 1649–1665. doi:10.1080/07391102.2017.1331864

Brovarets', O. O., Yurenko, Y. P., Dubey, I. Y., & Hovorun, D. M. (2012). Can DNA-binding proteins of replisome tautomerize nucleotide bases? *Ab initio* model study. *Journal of Biomolecular Structure & Dynamics, 29*, 1101–1109. doi:10.1080/07391102.2011.672624

Brovarets', O. O., Yurenko, Y. P., & Hovorun, D. M. (2013). Intermolecular CH•••O/N H-bonds in the biologically important pairs of natural nucleobases: A thorough quantum-chemical study. *Journal of Biomolecular Structure & Dynamics, 32*, 993–1022. doi:10.1080/07391102.2013.799439

Brovarets', O. O., Yurenko, Y. P., & Hovorun, D. M. (2015). The significant role of the intermolecular CH•••O/N hydrogen bonds in governing the biologically important pairs of the DNA and RNA modified bases: A comprehensive theoretical investigation. *Journal of Biomolecular Structure & Dynamics, 33*, 1624–1652. doi:10.1080/07391102.2013.799439

Brovarets', O. O., Zhurakivsky, R. O., & Hovorun, D. M. (2013a). The physico-chemical "anatomy" of the tautomerisation through the DPT of the biologically important pairs of hypoxanthine with DNA bases: QM and QTAIM perspectives. *Journal of Molecular Modeling, 19*, 4119–4137. doi:10.1007/s00894-012-1720-9

Brovarets', O. O., Zhurakivsky, R. O., & Hovorun, D. M. (2013b). DPT tautomerization of the long A•A* Watson-Crick base pair formed by the amino and imino tautomers of adenine: Combined QM and QTAIM investigation. *Journal of Molecular Modeling, 19*, 4223–4237. doi:10.1007/s00894-013-1880-2

Brovarets', O. O., Zhurakivsky, R. O., & Hovorun, D. M. (2013). The physico-chemical mechanism of the tautomerisation *via* the DPT of the long Hyp*·Hyp Watson– Crick base pair containing rare tautomer: A QM and QTAIM detailed look. *Chemical Physics Letters, 578*, 126–132. doi:10.1016/j.cplett.2013.05.067

Brovarets', O. O., Zhurakivsky, R. O., & Hovorun, D. M. (2014a). Structural, energetic and tautomeric properties of the T·T*/T*·T DNA mismatch involving mutagenic tautomer of thymine: A QM and QTAIM insight. *Chemical Physics Letters, 592*, 247–255. doi:10.1016/j.cplett.2013.12.034

Brovarets', O. O., Zhurakivsky, R. O., & Hovorun, D. M. (2014b). Does the tautomeric status of the adenine bases change upon the dissociation of the A*·A_{syn} Topal-Fresco DNA mismatch? A combined QM and QTAIM atomistic insight. *Physical Chemistry Chemical Physics, 16*, 3715–3725. doi:10.1039/c3cp54708f

Brovarets', O. O., Zhurakivsky, R. O., & Hovorun, D. M. (2014c). Is the DPT tautomerization of the long A·G Watson-Crick DNA base mispair a source of the adenine and guanine mutagenic tautomers? A QM and QTAIM response to the biologically important question. *Journal of Computational Chemistry, 35*, 451–466. doi:10.1002/jcc.23515

Brovarets', O. O., Zhurakivsky, R. O., & Hovorun, D. M. (2014d). A QM/QTAIM microstructural analysis of the tautomerisation *via* the DPT of the hypoxanthine·adenine nucleobase pair. *Molecular Physics, 112*, 2005–2016. doi:10.1080/00268976.2013.877170

Brovarets', O. O., Zhurakivsky, R. O., & Hovorun, D. M. (2015). DPT tautomerisation of the wobble guanine·thymine DNA base mispair is not mutagenic: QM and QTAIM arguments. *Journal of Biomolecular Structure and Dynamics, 33*, 674–689. doi:10.1080/07391102.2014

Cerón-Carrasco, J. P., Cerezo, J., & Jacquemin, D. (2014). How DNA is damaged by external electric fields: Selective mutation *vs.* random degradation. *Physical Chemistry Chemical Physics, 16*, 8243–8246. doi:10.1039/C3CP54518K

Cerón-Carrasco, J. P., & Jacquemin, D. (2013a). Electric field induced DNA damage: An open door for selective mutations. *Chemical Communications, 49*, 7578–7580. doi:10.1039/C3CC42593B

Cerón-Carrasco, J. P., & Jacquemin, D. (2013b). Electric-field induced mutation of DNA: A theoretical investigation of the GC base pair. *Physical Chemistry Chemical Physics, 15*, 4548–4553. doi:10.1039/C2CP44066K

Danilov, V. I., Anisimov, V. M., Kurita, N., & Hovorun, D. (2005). MP2 and DFT studies of the DNA rare base pairs: The molecular mechanism of the spontaneous substitution mutations conditioned by tautomerism of bases. *Chemical Physics Letters, 412*, 285–293. doi:10.1016/j.cplett.2005.06.123

Danilov, V. I., & Kventsel, G. F. (1971). *Electronic representations in the point mutation theory*. Kyiv: Naukova Dumka.

Duarte, F., Vöhringer-Martinez, E., & Toro-Labbé, A. (2011). Insights on the mechanism of proton transfer reactions in amino acids. *Physical Chemistry Chemical Physics, 13*, 7773–7782. doi:10.1039/c0cp02076a

Eigen, M. (1964). Proton transfer, acid-base catalysis, and enzymatic hydrolysis. Part I: Elementary processes. *Angewandte Chemie International Edition, 3*, 1–19. doi:10.1002/anie.196400011

Espinosa, E., Molins, E., & Lecomte, C. (1998). Hydrogen bond strengths revealed by topological analyses of experimentally observed electron densities. *Chemical Physics Letters, 285*, 170–173. doi:10.1016/S0009-2614(98)00036-0

Florian, J., Hrouda, V., & Hobza, P. (1994). Proton transfer in the adenine-thymine base pair. *Journal of the American Chemical Society, 116*, 1457–1460. doi:10.1021/ja00083a034

Gorb, L., Podolyan, Y., Dziekonski, P., Sokalski, W. A., & Leszczynski, J. (2004). Double-proton transfer in adenine−thymine and guanine−cytosine base pairs. A post-hartree−fock *ab initio* study. *Journal of the American Chemical Society, 126*, 10119–10129. doi:10.1021/ja049155n

Govorun, D. M., Danchuk, V. D., Mishchuk, Y. R., Kondratyuk, I. V., Radomsky, N. F., & Zheltovsky, N. V. (1992). AM1 calculation of the nucleic acid bases structure and vibrational spectra. *Journal of Molecular Structure, 267*, 99–103. doi:10.1016/0022-2860(92)87016-O

Guzmán-Angel, D., Inostroza-Rivera, R., Gutiérrez-Oliva, S., Herrera, B., & Toro-Labbé, A. (2016). Role of water in intramolecular proton transfer reactions of formamide and thioformamide. *Theoretical Chemistry Accounts, 135*, 617. doi:10.1007/s00214-015-1774-8

Hargis, J. C., Vöhringer-Martinez, E., Woodcock, H. L., Toro-Labbé, A., & Schaefer, H. F., 3rd (2011). Characterizing the mechanism of the double proton transfer in the formamide dimer. *Journal of Physical Chemistry A, 115*, 2650–2657. doi:10.1021/jp111834v

Hovorun, D. M. (1997). A structural isomerism of nucleotide bases: AM1 calculation. *Biopolymers & Cell, 13*, 127–134. doi:10.7124/bc.000474

Hovorun, D. M., Gorb, L., & Leszczynski, J. (1999). From the nonplanarity of the amino group to the structural nonrigidity of the molecule: A post-Hartree-Fock *ab initio* study of 2-aminoimidazole. *International Journal of Quantum*

Chemistry, 75, 245–253. doi:10.1002/(SICI)1097-461X(1999)75:3<245::AID-QUA14>3.0.CO;2-0

Hratchian, H. P., & Schlegel, H. B. (2005). Finding minima, transition states, and following reaction pathways on *ab initio* potential energy surfaces. In Dykstra, C. E., Frenking, G., Kim, K. S., & Scuseria, G. (Eds.), *Theory and applications of computational chemistry: The first 40 years* (pp. 195-249). Amsterdam: Elsevier. doi:10.1016/B978-044451719-7/50053-6

Inostroza-Rivera, R., Yahia-Ouahmed, M., Tognetti, V., Joubert, L., Herrera, B., & Toro-Labbé, A. (2015). Atomic decomposition of conceptual DFT descriptors: Application to proton transfer reactions. *Physical Chemistry Chemical Physics, 17*, 17797–17808. doi:10.1039/C5CP01515D

Jacquemin, D., Zúñiga, J., Requena, A., & Céron-Carrasco, J. P. (2014). Assessing the importance of proton transfer reactions in DNA. *Accounts of Chemical Research, 47*, 2467–2474. doi:10.1021/ar500148c

Jaque, P., Toro-Labbé, A., Politzer, P., & Geerlings, P. (2008). Reaction force constant and projected force constants of vibrational modes along the path of an intramolecular proton transfer reaction. *Chemical Physics Letters, 456*, 135–140. doi:10.1016/j.cplett.2008.03.054

Jin, L., Lv, M., Zhao, M., Wang, R., Zhao, C., Lu, J., … Wei, Y. (2017). Formic acid catalyzed isomerization of protonated cytosine: A lower barrier reaction for tautomer production of potential biological importance. *Physical Chemistry Chemical Physics, 19*, 13515–13523. doi:10.1039/c7cp01008 g

Jin, L., Shi, Sh, Zhao, Y., Luo, L., Zhao, C., Lu, J., & Jiang, M. (2018). Effects of C5-substituent group on the hydrogen peroxide-mediated tautomerisation of protonated cytosine: A theoretical perspective. *Molecular Physics, 116*, 471–481. doi:10.1080/00268976.2017.1406159

Karran, P., & Lindahl, T. (1980). Hypoxanthine in deoxyribonucleic acid: Generation by heat-induced hydrolysis of adenine residues and release in free form by a deoxyribonucleic acid glycosylase from calf thymus. *Biochemistry, 19*, 6005–6011. doi:10.1021/bi00567a010

Kirby, A. J. (1997). Efficiency of proton transfer catalysis in models and enzymes. *Accounts of Chemical Research, 30*, 290–296. doi:10.1021/ar960056r

Koch, M., Pagan, M., Persson, M., Gawinkowski, S., Waluk, J., & Kumagai, T. (2017). Direct observation of double hydrogen transfer *via* quantum tunneling in a single porphycene molecule on a Ag(110) surface. *Journal of the American Chemical Society, 139*, 12681–12687. doi:10.1021/jacs.7b06905

Kondratyuk, I. V., Samijlenko, S. P., & Kolomiets', I. M., & Hovorun, D. M. (2000). Prototropic molecular-zwitterionic tautomerism of xanthine and hypoxanthine. *Journal of Molecular Structure, 523*, 109–118. doi:10.1016/S0022-2860(99)00385-3

Löwdin, P.-O. (1963). Proton tunneling in DNA and its biological implications. *Reviews in Modern Physics, 35*, 724–732. doi:10.1103/RevModPhys.35.724

Löwdin, P.-O. (1966). Quantum genetics and the aperiodic solid: Some aspects on the biological problems of heredity, mutations, aging, and tumors in view of the quantum theory of the DNA molecule. In P.-O. Löwdin (Ed.), *Advances in Quantum Chemistry* (pp. 213–360). New York, NY: Academic Press. Retrieved from http://www.researchgate.net/publication/235183358_QUANTUM_GENETICS_AND_THE_APERIODIC_SOLID_SOME_ASPECTS_ON_THE_BIOLOGICAL_PROBLEMS_OF_HEREDITY_MUTATIONS_AGEING_AND_TUMORS_IN_VIEW_OF_THE_QUANTUM_THEORY_OF_THE_DNA_MOLECULE

Lozynski, M., Rusinska-Roszak, D., & Mack, H.-G. (1998). Hydrogen bonding and density functional calculations: The B3LYP approach as the shortest way to MP2 results. *Journal of Physical Chemistry A, 102*, 2899–2903. doi:10.1021/jp973142x

Markova, N., Pejov, L., Stoyanova, N., & Enchev, V. (2017). Hybrid MC/QC simulations of water-assisted proton transfer in nucleosides. Guanosine and its analog acyclovir. *Journal of Biomolecular Structure and Dynamics, 35*, 1168–1188. doi:10.1080/07391102.2016.1179594

Mata, I., Alkorta, I., Espinosa, E., & Molins, E. (2011). Relationships between interaction energy, intermolecular distance and electron density properties in hydrogen bonded complexes under external electric fields. *Chemical Physics Letters, 507*, 185–189. doi:10.1016/j.cplett.2011.03.055

Matta, C. F. (2010). How dependent are molecular and atomic properties on the electronic structure method? Comparison of Hartree-Fock, DFT, and MP2 on a biologically relevant set of molecules. *Journal of Computational Chemistry, 31*, 1297–1311. doi:10.1002/jcc.21417

Matta, C. F., & Boyd, R. J. (2007). *The quantum theory of Atoms in Molecules: From solid state to DNA and drug design*. KGaA: Wiley-VCH Verlag GmbH & Co.

Matta, C. F., Castillo, N., & Boyd, R. J. (2006). Extended weak bonding interactions in DNA: π-Stacking (base-base), base-backbone, and backbone-backbone interactions. *Journal of Physical Chemistry B, 110*, 563–578.

Maximoff, S. N., Kamerlin, Sh. C. L., & Florian, J. (2017). DNA polymerase λ active site favors a mutagenic mispair between the enol form of deoxyguanosine triphosphate substrate and the keto form of thymidine template: A free energy perturbation study. *Journal of Physical Chemistry B, 121*, 7813–7822. doi:10.1021/acs.jpcb.7b04874

Mertz, E. L., & Krishtalik, L. I. (2000). Low dielectric response in enzyme active site. *Proceedings of the National Academy of Sciences of USA, 97*, 2081–2086. doi:10.1073/pnas.050316997

Murray, J. S., Toro-Labbé, A., Clark, T., & Politzer, P. (2009). Analysis of diatomic bond dissociation and formation in terms of the reaction force and the position-dependent reaction force constant. *Journal of Molecular Modeling, 15*, 701–706. doi:10.1007/s00894-008-0400-2

Nikolaienko, T. Y., Bulavin, L. A., & Hovorun, D. M. (2011). How flexible are DNA constituents? The quantum-mechanical study. *Journal of Biomolecular Structure & Dynamics, 29*, 563–575. doi:10.1080/07391102.2011.10507406

Padermshoke, A., Katsumoto, Y., Masaki, R., & Aida, M. (2008). Thermally induced double proton transfer in GG and wobble GT base pairs: A possible origin of the mutagenic guanine. *Chemical Physics Letters, 457*, 232–236. doi:10.1016/j.cplett.2008.04.029

Palafox, M. A., & Rastogi, V. K. (2016). Density functional computations on 6-aminouracil: Effect of amino group in the 6th position on the Watson-Crick base pair uridine–adenosine. *Australian Journal of Chemistry, 69*, 881–889. doi:10.1071/CH15793

Petrushka, J., Sowers, L. C., & Goodman, M. (1986). Comparison of nucleotide interactions in water, proteins, and vacuum: Model for DNA polymerase fidelity. *Proceeding of the National Academy of Sciences of USA, 83*, 1559–1562. doi:10.1073/pnas.83.6.1559

Platonov, M. O., Samijlenko, S. P., Sudakov, O. O., Kondratyuk, I. V., & Hovorun, D. M. (2005). To what extent can methyl derivatives be regarded as stabilized tautomers of xanthine? *Spectrochimica Acta, Part A: Molecular and Biomolecular Spectroscopy, 62*, 112–114. doi:10.1016/j.saa.2004.12.012

Politzer, P., Murray, J. S., & Jaque, P. (2013). Perspectives on the reaction force constant. *Journal of Molecular Modeling, 19*, 4111–4118. doi:10.1007/s00894-012-1713-8

Romero, E. E., & Hernandez, F. E. (2017). Solvent effect on the intermolecular proton transfer of the Watson and Crick guanine-cytosine and adenine-thymine base pairs: A polarizable continuum model study. *Physical Chemistry Chemical Physics, 20*, 1198–1209.

Ronen, A. (1980). 2-Aminopurine. *Mutation Research/Reviews in Genetic Toxicology, 75*, 1–47. doi:10.1016/0165-1110(80)90026-3

Roßbach, S., & Ochsenfeld, Ch. (2017). Influence of coupling and embedding schemes on QM size convergence in QM/MM approaches for the example of a proton transfer in DNA. *Journal of Chemical Theory and Computation, 13*, 1102–1107.

Ruiz-Blanco, Y. B., Almeida, Y., Sotomayor-Torres, C. M., & García, Y. (2017). Unveiled electric profiles within hydrogen bonds suggest DNA base pairs with similar bond strengths. *PLoS One, 12*, e0185638. doi:10.1371/journal.pone.0185638

Saenger, W. (1984). *Principles of nucleic acid structure*. New York, NY: Springer.

Samijlenko, S. P., Krechkivska, O. M., Kosach, D. A., & Hovorun, D. M. (2004). Transitions to high tautomeric states can be induced in adenine by interactions with carboxylate and sodium ions: DFT calculation data. *Journal of Molecular Structure, 708*, 97–104. doi:10.1016/j.molstruc.2004.05.034

Scheiner, S. (1994). Bent hydrogen bonds and proton transfers. *Accounts of Chemical Research, 27*, 402–408. doi:10.1021/ar00048a003

Shaik, S., Mandal, D., & Ramanan, R. (2016). Oriented electric fields as future smart reagents in chemistry. *Nature Chemistry, 8*, 1091–1098. doi:10.1038/nchem.2651

Shi, Y., Jiang, W., Zhang, Z., & Wang, Z. (2017). Cooperative vibrational properties of hydrogen bonds in Watson-Crick DNA base pairs. *New Journal of Chemistry, 41*, 12104–12109. doi:10.1039/C7NJ03088F

Smedarchina, Z., Siebrand, W., & Fernández-Ramos, A. (2018). Entanglement and co-tunneling of two equivalent protons in hydrogen bond pairs. *Journal of Chemical Physics, 148*, 102307–1–102307-15. doi:10.1063/1.5000681

Sowlati-Hashjin, Sh., & Matta, C. F. (2013). The chemical bond in external electric fields: Energies, geometries, and vibrational Stark shifts of diatomic molecules. *Journal of Chemical Physics, 139*, 144101–1–144101-14. doi:10.1063/1.4820487

Strazewski, P., & Tamm, C. (1990). Replication experiments with nucleotide base analogues. *Angewandte Chemie International Edition, 29*, 36–57. doi:10.1002/anie.199000361

Tolosa, S., Sansón, J. A., & Hidalgo, A. (2017). Theoretical thermodynamic study of the adenine–thymine tautomeric equilibrium: Electronic structure calculations and steered molecular dynamic simulations. *International Journal of Quantum Chemistry, 117*, e25429. doi:10.1002/qua.25429

Tolosa, S., Sansón, J. A., & Hidalgo, A. (2018). Mechanisms for guanine–cytosine tautomeric equilibrium in solution *via* steered molecular dynamic simulations. *Journal of Molecular Liquids, 251*, 308–316. doi:10.1016/j.molliq.2017.12.091

Toro-Labbé, A., Gutiérrez-Oliva, S., Murray, J. S., & Politzer, P. (2009). The reaction force and the transition region of a reaction. *Journal of Molecular Modeling, 15*, 707–710. doi:10.1007/s00894-008-0431-8

Toro-Labbé, A., Gutierrez-Oliva, S., Concha, M. C., Murray, J. S., & Politzer, P. (2004). Analysis of two intramolecular proton transfer processes in terms of the reaction force. *Journal of Chemical Physics, 121*, 4570–4576. doi:10.1063/1.1777216

Wang, W., Hellinga, H. W., & Beese, L. S. (2011). Structural evidence for the rare tautomer hypothesis of spontaneous mutagenesis. *Proceeding of the National Academy of Sciences of USA, 108*, 17644–17648. doi:10.1073/pnas.1114496108

Ward, D. C., Reich, E., & Stryer, L. (1969). Fluorescence studies of nucleotides and polynucleotides: I. Formycin, 2-aminopurine riboside, 2,6-diaminopurine riboside, and their derivatives. *Journal of Biological Chemistry, 244*, 1228–1237. Retrieved from http://www.jbc.org/content/244/5/1228.abstract

Yang, F., Wu, R.-Z., Yan, C.-X., Yang, X., Zhou, D.-G., & Zhou, P.-P. (2017). Quantitative relationships between bond lengths, stretching vibrational frequencies, bond force constants, and bond orders in the hydrogen-bonded complexes involving hydrogen halides. *Structural Chemistry, 29*, 513–521. doi:10.1007/s11224-017-1048-2

Yepes, D., Murray, J. S., Politzer, P., & Jaque, P. (2012). The reaction force constant: An indicator of the synchronicity in double proton transfer reactions. *Physical Chemistry Chemical Physics, 14*, 11125–11134. doi:10.1039/c2cp41064 h

Yepes, D., Murray, J. S., Santos, J. C., Toro-Labbé, A., Politzer, P., & Jaque, P. (2013a). Fine structure in the transition region: Reaction force analyses of water-assisted proton transfers. *Journal of Molecular Modeling, 19*, 2689–2697. doi:10.1007/s00894-012-1475-3

Yepes, D., Murray, J. S., Santos, J. C., Toro-Labbé, A., Politzer, P., & Jaque, P. (2013b). Fine structure in the transition region: Reaction force analyses of water-assisted proton transfers. *Journal of Molecular Modeling, 19*, 2689–2697. doi:10.1007/s00894-012-1475-3

Zhang, G., & Xie, S. (2016). External electric field promotes proton transfer in the radical cation of adenine–thymine. *Modern Physics Letters B, 30*, 1650276. doi:10.1142/S0217984916502766